

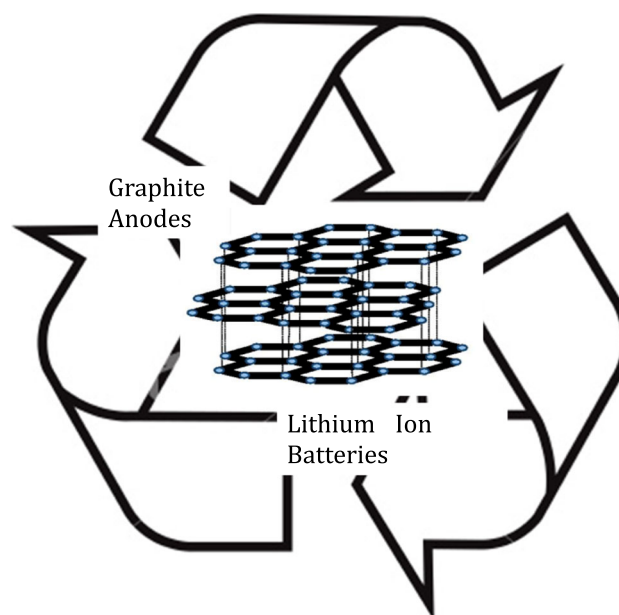
Recycling of graphite anodes for the next generation of lithium ion batteries

Bahar Moradi¹ · Gerardine G. Botte¹

Received: 8 March 2015 / Accepted: 16 December 2015 / Published online: 28 December 2015
© Springer Science+Business Media Dordrecht 2015

Abstract Graphite is currently the state-of-the-art anode material for most of the commercial lithium ion batteries. Among different types of natural graphite, flake graphite has been recently recognized as one of the critical materials due to the predicted future market growth of lithium ion batteries for vehicular applications. Current status and future demand of flake graphite in the market are discussed. It was found that flake graphite could become a critical material in the near future for countries such as the United States and members of the European Union with no graphite production. Recycling of flake graphite from its different waste resources is proposed as a potential solution to meet the future demand of graphite. The current status of graphite anodes in the present recycling technologies of spent lithium ion batteries was reviewed. The limitation of current technologies and a new perspective towards the future concept of “battery recycling” were also pointed out. Challenges in recycling battery grade flake graphite from spent lithium ion batteries and possible research opportunities in this regard were introduced.

Graphical Abstract



Keywords Lithium ion batteries · Graphite recycling · Surface modification · Solid electrolyte interface · Capacity fade

1 Introduction

World demand for lithium ion batteries (LIBs) as the energy source for cell phones, laptops, power tools, medical equipment, entertainment devices, and the automobile industry has shown a rapid growth over the past two decades [1]. Low self-discharge rate, high rate capacity (1C),

✉ Gerardine G. Botte
botte@ohio.edu

¹ Chemical and Biomolecular Engineering Department, Center for Electrochemical Engineering Research, 182 Mill St., Athens, OH 45701, USA

excellent cycling behavior (>1200 cycles), high energy density, temperature tolerance, long life-time, and no “memory effect” are the advantages that LIBs offer over other batteries [2]. Apart from portable devices, a considerable market growth is predicted for LIBs in the future as part of the automobile industry where they are used to power hybrid electrical vehicles (HEVs), and electrical vehicles (EVs) [3]. Many companies such as Audi, Toshiba-Mitsubishi JV, BMW, Ford, Honda, General Motors, Nissan, Toyota, and Mercedes Benz have already announced launching in the market lithium-ion powered automobiles [4]. Many researchers and consulting firms have published reports that forecasts LIBs market growth. Merrill Lynch estimates that the LIBs market will reach \$70 billion by 2020 while the Boston Consulting Group predicts that the market for EV LIBs alone will reach \$25 billion by then [5].

Most of the LIBs being used in portable devices use a material such as LiM_xO_x as cathode. For example, $\text{LiNi}_{0.8}\text{Co}_{0.15}\text{Al}_{0.05}\text{O}_2$ is the cathode of the LIBs in cell phones, cameras, and laptops. LiMn_2O_4 , $\text{LiCo}_{1/3}\text{Ni}_{1/3}\text{Mn}_{1/3}\text{O}_2$, and LiFePO_4 are the cathode materials for power tools, medical equipment, HEVs, Plug-in HEVs, and EVs [4, 6, 7]. Till date, the anode in most of the commercial LIBs is graphite since it stores lithium ion well when the battery is charged and has a long-term cycle stability [8]. LIBs' electrolytes are lithium salts (such as LiClO_4 , LiNiO_2 and LiPF_6) dissolved in organic solvents [9–12]. Other parts of the LIBs are binder, current collectors (copper and aluminum), plastics, steel, and thermal insulation. The estimated weight composition of the materials in the battery is 5–20 % cobalt, 5–10 % nickel, 5–7 % lithium, 15 % organic chemicals, 7 % plastics, 12–21 % carbon, and the remaining weight is related to copper, aluminum, and steel [6, 7, 13].

Currently, some of the main challenges of LIB technology are the overall production cost and the long-term material supply for future demand. Cost of the materials being used in a lithium ion cell is at least 33 % of the production cost mainly because of expensive raw materials such as cobalt, lithium, nickel, and manganese [14]. Moreover, the primary resources of these metals are limited around the world, while the amounts of easily minable metal ores are in decline [15]. In addition to the metallic compounds used in LIBs, and their cost, it is important to consider the supply of graphite as the commercial anode material for LIBs because a lithium ion cell contains at least 11 times more graphite than lithium depending on the battery type and application [6, 16]. For example, Table 1 summarizes the content of lithium and graphite in LIBs with LiMn_2O_4 cathode for HEVs, Plug-in HEVs, and EVs. The content of graphite in mid size HEVs, PHEVs, and EVs can approximately reach up to ~4, 8, and 47 kg, respectively, and in HEVs, PHEVs, and EVs sport utility vehicles (SUVs) up to ~5, 21, and 65 kg, respectively

[6, 7]. Using the values reported above, and the data from vehicle sales during the first six months of 2014 in the United States (287,761 vehicles from January 1st to June 31st 2014 [17]), graphite consumption would be at least 1.6×10^4 metric ton for year 2014 in the automobile industry alone [6, 7, 17].

The increasing worldwide demand of graphite started from the last half of 2009 and its growth was steady throughout 2012 and into 2013. This increase is predicted to continue mainly due to conversion from nickel-metal hydride batteries to LIBs and the growth of the LIBs sector for vehicles [18]. In 2010, the global market for natural flake graphite was estimated to be around half of million metric ton per year [19, 20]. Based on industrial analysis, this demand could potentially exceed one million metric ton per year by 2020 [21, 22]. Accordingly, the growth of EVs in upcoming years is expected to coincide with a dramatic raise in the graphite cost. Only from 2009 to 2013, the cost of imported flake graphite to the United States increased more than 100 % [18]. This evidence indicates that in the near future graphite would be in the list of the most critical materials for high performance LIBs.

From an economical point of view, a possible solution to meet future supply of raw materials necessary for LIBs production is through recycling of the battery components to the grade that could be reused in LIBs. Although, several companies in the United States, Asia, Europe, and Canada are currently recycling battery scraps to recover some valuable materials, the focus has been on the recovery of the cathode components for LIBs. Not much effort has been dedicated to the recycling and reusing of graphite in the LIBs. Within this context, this paper presents a review of recycling technologies for graphite in LIBs, challenges, and opportunities that can be enable by new processes such as the use of surface modified anode materials.

2 Battery grade graphite

Graphite is the most commonly used anode material in commercial LIBs due to its stable thermal and mechanical structure, electrical conductivity, non-toxicity, abundance, and prevention of dendrites formation in the battery [2, 23]. However, in the LIBs field, using the term “Graphite” may not be precise enough since not all kinds of naturally mined graphite can be used in these batteries. This section presents a review of the type of graphite grades that are used in LIBs.

2.1 Natural graphite

In general, differing in purity and morphology, there are three different types of natural graphite (NG): (1)

Table 1 Graphite and lithium content for HEV, PHEV, and EV lithium ion batteries using LiMnO_4 as cathode material [6, 7]

Component	Mass (Kg)					
	Mid-size vehicles			Sport utility vehicles		
	HEV	PHEV	EV	HEV	PHEV	EV
Graphite	4.08	8.35	47.40	4.80	21.00	64.65
Li as cathode active material	0.37	0.76	4.22	0.44	1.99	5.76
Graphite to Li ratio	11.02	10.98	11.23	10.90	10.55	11.22
Mass of battery pack	34.00	67.00	316.00	40.00	176.00	431.00

Mass ratio of graphite to lithium is at least 10 times larger

amorphous, (2) flake, and (3) vein graphite. Amorphous graphite has the lowest carbon purity ranging between 60 and 90 % and its flake plates are relatively small in size [24]. Flake graphite is 75–97 % pure and highly crystallized with isolated, flat, plate-like particles [25, 26]. Vein (lump) graphite occurs mainly in Sri Lanka. It has the highest purity ranging between 98 and 99.9 % and the highest crystallinity ranging from flaky to fine powders [26–29]. Table 2 summarizes the classification of NG based on flake size and carbon purity as reported by LIB-ERTAS group [16].

Since the battery grade graphite should be highly pure and crystallized with large flake sizes [26], only flake and vein graphite can be used as the raw material for anodes in LIBs due to their high degree of graphitization [30]. However, vein graphite is mined commercially in a few countries and has a limited availability. Therefore, it is relatively expensive and not abundant enough to be considered as a source of raw material for LIBs. As a result, practically, flake graphite is the main natural source of graphite for producing battery grade graphite [16]. Figure 1 shows a scanning electron micrograph (SEM) of the flaky morphology of natural flake graphite (NFG). NFG has a layered structure. In each layer, the carbon atoms are arranged in a honeycomb lattice and the distance between the planes is 0.37 nm. A distribution of graphite flake sizes can be seen in the micrograph. Graphite particles mostly have prismatic platelets and the basal planes and edge dimensions are well-defined.

However, NFG cannot be used directly in advanced LIBs, because (1) NFG is not pure enough for battery

applications [31]; and (2) NFGs are not isotropic, i.e. the dimensions of NG flakes in the parallel and perpendicular directions to the basal planes are not the same. This type of morphology adversely affects uniform distribution of the particles on the current collector. Furthermore, NG flakes tend to adhere to the current collector with the basal-plane surface in the direction of the current flow and with edge-plane surface vertical to the current flow. Figure 2 shows the SEM images of basal and edge planes of NFG and the schematic of highly oriented NFG coated on a copper foil. As a result of this orientation, it becomes more difficult for Li^+ to intercalate into the graphite structure since the intercalation of Li^+ occurs through edge-plane surfaces. Subsequently, NFG demonstrates poor rate capacity. Therefore, upgrading processes are necessary to provide highly pure NFG and solve the problem of low rate capacity due to the high orientation of NG flakes.

The upgrading processes of NFG include (1) purification steps by different methods such as heat treatment [32, 33] and chemical treatment [31], and (2) rolling of the graphite flakes into a spherical shape by different mechanical methods. In the mechanical methods, small NG pieces could be folded into a compact ball by pressure from both sides of the planar graphite fragments. Figure 3 shows the structure and morphology of spherical graphite. The end product of upgrading flake graphite is potato-shape type particles with more than 99.9 % carbon purity, which is known as spherical graphite [34–37]. Unfortunately, the yield of spherical graphite production is only 30 %, thus spherical graphite is three times more expensive when compared to flake graphite [16].

Table 2 General natural graphite properties [16]

Graphite product	Carbon content (%)	Graphite size (μm)
Large flake	94–97	>177
Medium flake	94–97	149–177
Fine flake	94–97	<149
Amorphous	80–85	≥ 37

Fine and medium flakes graphite types are used in graphite electrode production predominantly

2.2 Synthetic graphite

Apart from NG resources, the demand for graphite is fulfilled with synthetic graphite (SG), especially for those countries with limited or no NFG resources. SG is produced by heat treatment of unstructured carbon such as crushed calcined petroleum coke and coal tar pitch at temperatures as high as 2500 °C under exclusion of oxygen. Using high temperatures, disordered layers of the

Fig. 1 Scanning electron microscopy images of natural flake graphite. Particle size **a** 20 μm ; **b** 40 μm . Reproduced with permission [185]. **c** Schematic illustration of carbon atoms and graphene layers arrangement in the structure of graphite

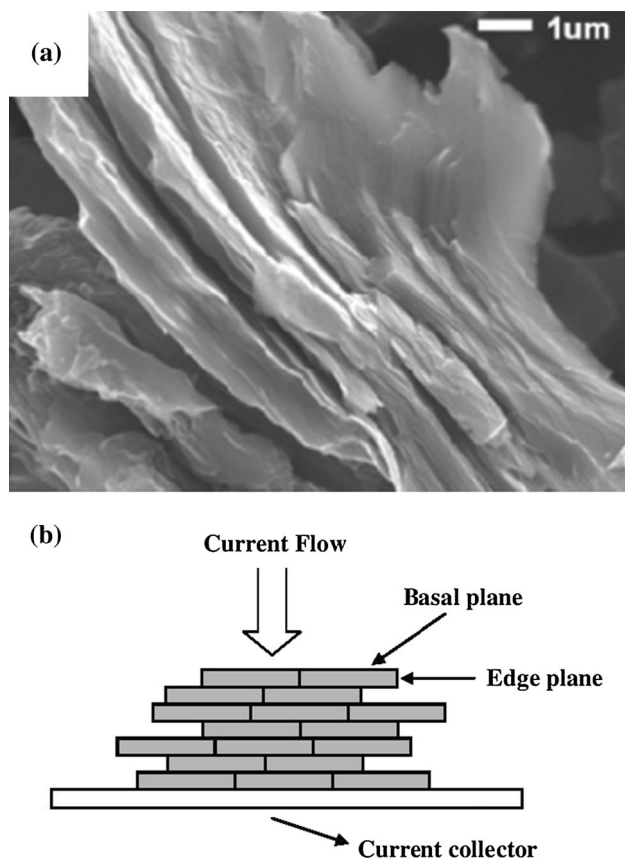
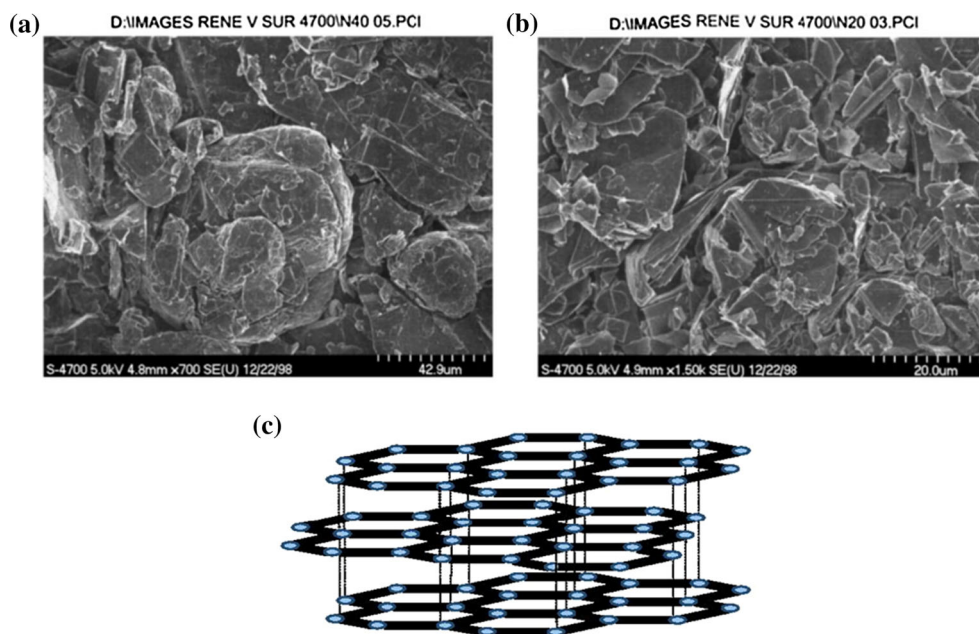
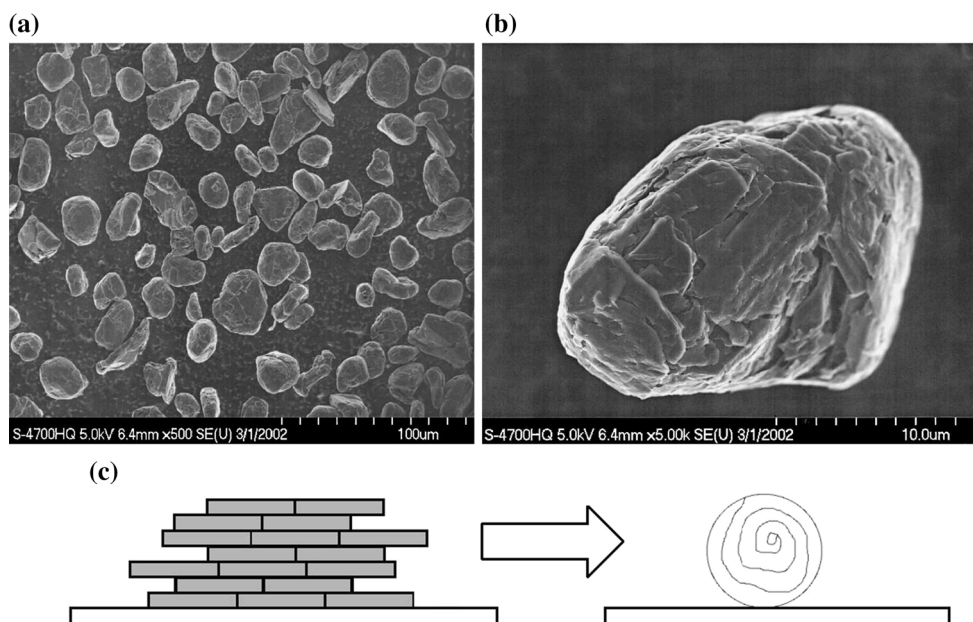


Fig. 2 **a** Scanning electron microscopy images showing basal and edge planes. Reproduced with permission [186], **b** schematic views of the raw natural graphite flakes spread on copper current collector. The basal and edge planes are parallel and perpendicular to the current collector, respectively [35]

carbon source become orientated similar to the graphitic structure. One of the biggest advantages of the SG is that it contains significantly lower impurities than the original carbon source due to the high temperature used during the synthesis process [16, 26, 38]. The purity of the end product is usually as high as 97–99.9 % [39]. By using high-purity coke as raw material, purity levels above 99.9 % can be achieved as well [38]. The morphology of the end graphite ranges from fine and flaky powder to larger, fine size and irregular grains [16, 26]. Several different factors such as crystalline make-up, maximum heat-treatment temperature, and furnace processing atmosphere affect the electrochemical performance of the SG [40]. The electrochemical characteristics of SG anodes have been reported [41–44]. Aurbach et al. [43] performed a comparative study on the electrochemical behavior of SG and NFG as anode materials in propylene carbonate (PC) solutions for LIBs. Figure 4a shows the galvanostatic cycles of SG and two types of NFG. The irreversible capacity of the NFG electrodes is much smaller than that of the SG electrode. Two dimensional (2D) atomic force microscopy (AFM) images and in situ surface height profiles of NFG and SG during the first cathodic polarization show differences in the particle morphologies and their crystal structure (Fig. 4b). More intense changes in the height profile are observed in the SG electrode than in the NFG electrode. SG particles have a lot of crevices in their edge planes, thus the build-up of internal pressure due to PC reduction inside these crevices is pronounced. This increases their active surface area, resulting in bigger irreversible capacity. Hence, for NFG with smoother edge planes, the above

Fig. 3 Scanning electron microscopy images of **a** general view of potato-shape natural graphite. The particles show only a small variation in shape, **b** individual potato-shape natural graphite. Reproduced with permission [31]; **c** schematic illustration of spherical graphite production from NFG. The NFG particles are folded concentrically to form potato-shape graphite



unfavorable process is observed less and the irreversible capacity is relatively small [43].

SG accounts for a significant share of the graphite market, in particular in North America. In 2011 SG contributed 56 % to the global graphite market. The production of SG powder typically involves a small number of specialized producers in North America, Europe and Japan. However, its application as anode material for future demand of LIBs is limited by its price [45, 46] as the price of SG is usually 1.5–3 times higher than NFG with the same quality [16].

2.3 Expandable graphite

Expandable graphite (EG) is a special form of intercalated graphite with distinctive properties. The raw material for EG production is usually NFG. Basically, EG is graphite with dramatic enlarged distances between its graphene layers. The production of EG has two essential steps. Initially, flake graphite is intercalated by a type of strong oxidizing agent such as sulfuric acid to insert sulphate ions into the graphite's crystal lattice. The intercalation process can be done by chemical (CI) and electrochemical (EI) methods [47]. The end product of this step is called "graphite bisulphate". Then by immediate exposure to high temperatures, graphene sheets fall apart and graphite expands. Depending on the temperature, mildly or fully expanded graphite can be achieved. By using temperatures >800 °C during the heat treatment, graphite expands at least 300 times. As a result of this expansion, the surface area of graphite increases about 1000 times [16, 26]. Processing conditions such as oxidizing agent amount, heat

treatment temperature, and duration affect the structure of the EG. Figure 5 Electrochemical performance of the EG as anode materials for LIBs has been extensively investigated in the literature [48–50].

Bai et al. [49] performed a comparative study on EG and NFG as anode materials for LIBs via a variety of electrochemical testing techniques such as galvanic cycling. Figure 6a, and b show the galvanostatic cycles of the first three cycles of NFG and EG, respectively. The reversible capacity of EG is almost twice that of NFG. However, the first-cycle Coulombic efficiency and capacity retention of NFG is much larger than EG. The large irreversible capacity in EG comparing to NFG was attributed to the disorder-induced structure instability. Moreover, the second cycle curves of EG indicates smaller crystallite structure and high specific surface area. EG electrodes exhibit a broad electrochemical window as a function of lithium capacity and a large voltage hysteresis between discharge and charge voltage curves, which is more similar to the nongraphitic carbons. The kinetics properties of EG and NFG electrodes were also compared by Altering Current impedance measurements as shown in Fig. 6c, d. EG electrodes exhibit higher electrochemical activity during the charge and discharge process. The presence of functional groups at the unorganized carbon sites results in more irreversible lithium inserting in the electrode with the growth of cycle number, which could lead to the increase of electric conductivity of EG. On the contrary, for the NFG electrode, the radius of the semicircle in Fig. 6c increases with the cycle process, which is explained by the fact that the SEI on the surface of NFG electrode grows thicker with the cycle process [49].

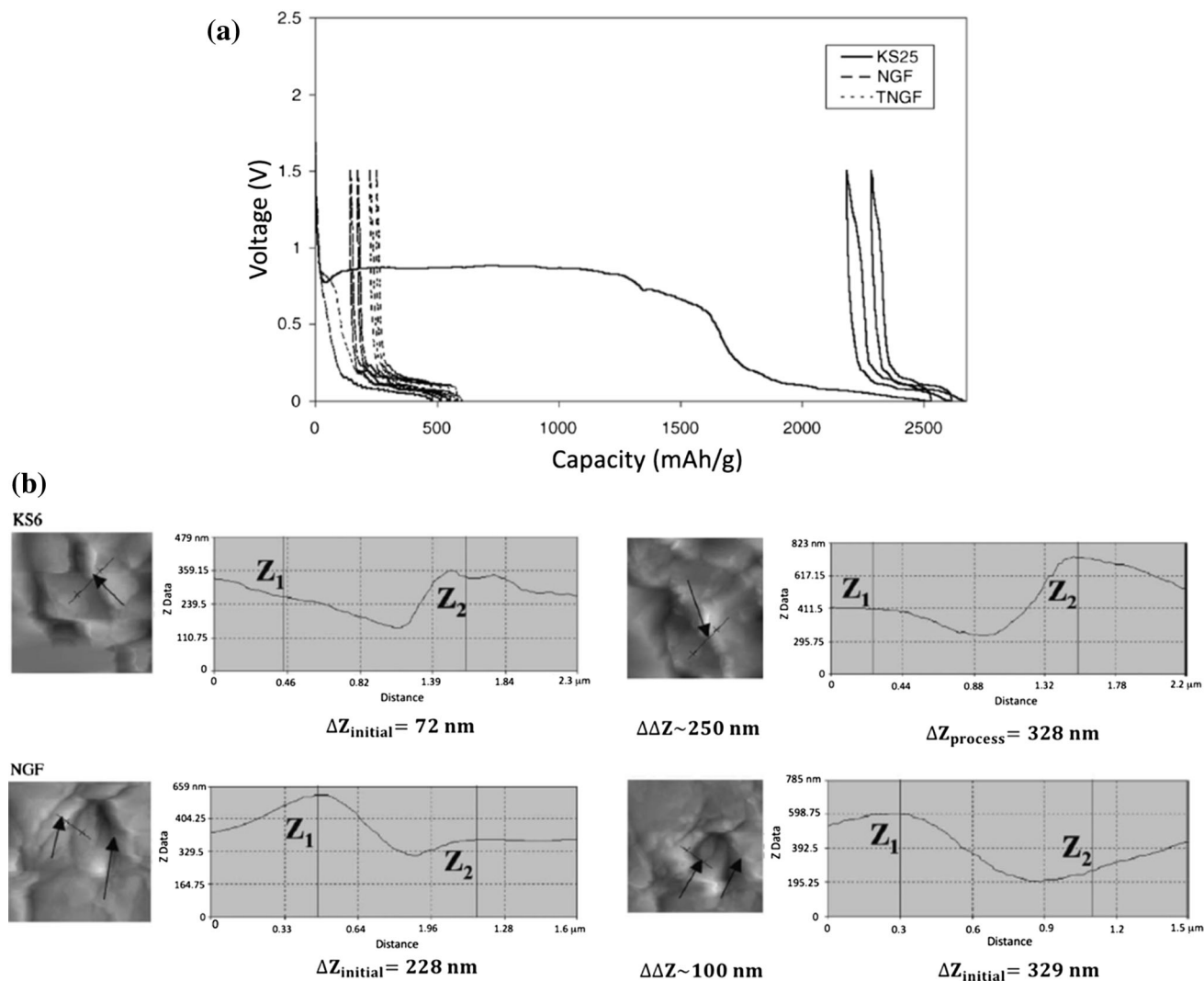


Fig. 4 **a** First consecutive discharge/charge cycles of electrodes comprised of synthetic graphite flakes (KS25), and two types of natural graphite flakes (NGF and TNGF) in EC:PC = 2:3/1 M LiClO₄ solutions. **b** 2D atomic force microscopy images of KS6 and NGF electrodes measured in situ during the first galvanostatic cathodic polarization in EC-PC/LiClO₄ solutions. The images were

obtained at constant potentials that the electrode reached during the process. Typical, selected height electrode profiles (ΔZ) are also presented. The height differences in the profiles for the initial and the polarized states are marked. $\Delta \Delta Z$ values marked near the images are the differences in ΔZ between the initial and polarized states. Reproduced with permission [43]

3 Market analysis

Worldwide demand for high quality NFG started to face a considerable raise since 2009. Based on Roskill Global Commodities market reports, annual demand growth of flake graphite will be 10–12 % per year from 2010 to 2016 mostly driven by the dramatic annual growth in the production of LIBs [51]. Mining and production of NG are limited to several countries around the world. Figure 7 represents the world NG producing countries in 2013. Among these countries, China, Canada, and Madagascar are the main suppliers of worldwide flake graphite [18, 29]. Besides, due to China's new policies in decreasing export rate of flake graphite and increasing utilization of China's

flake graphite to manufacture the end products, the price of flake graphite has raised more than 100 % and it is predicted that this will have remarkable effects on flake graphite's prices in the near future [39].

As a consequence, the United States and countries from the European Union with no graphite production deem flake graphite as a critical material [45, 52]. Accordingly, future supply of graphite has become a considerable concern for the United States due to the estimated dramatic future cost increase, being 100 % relied on importing flake graphite from other countries, and the fact that the United States plans to be one of the main manufacturer of EVs in the future. For example, it is expected that by 2015, the United States would have 1 million plug-in hybrid vehicles

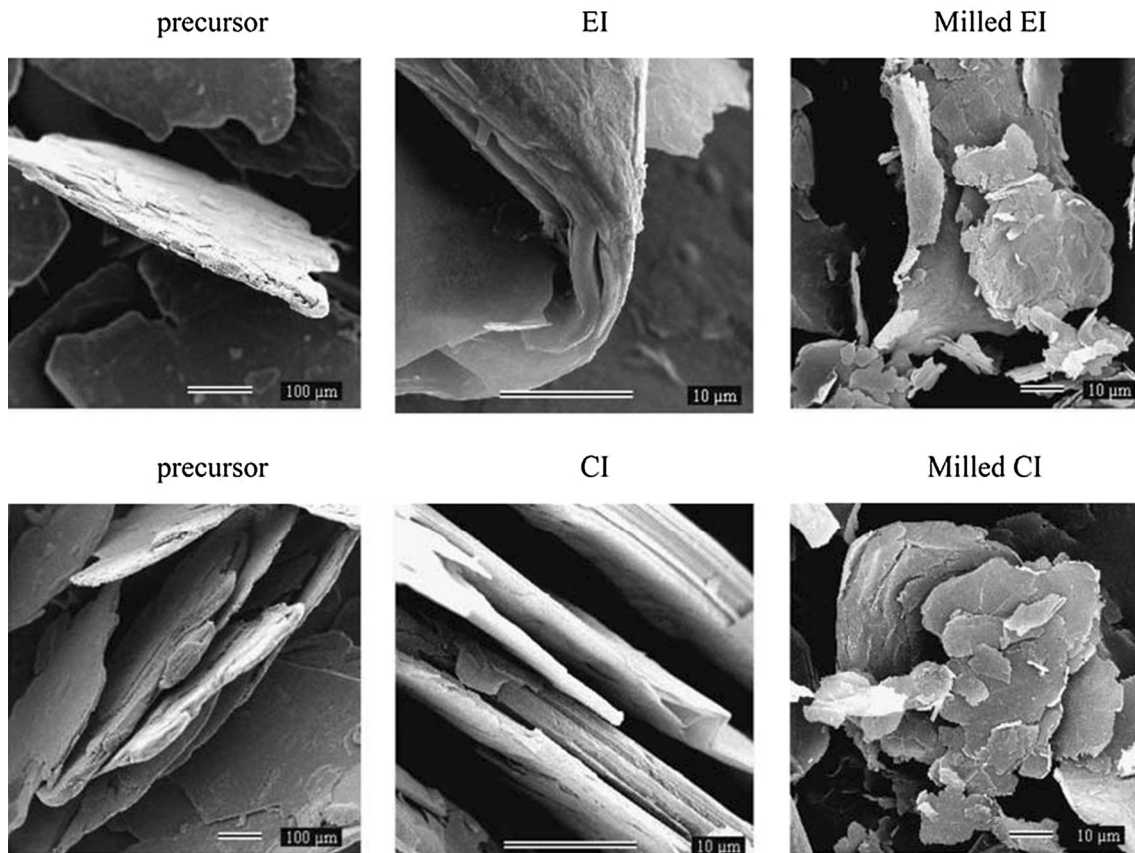


Fig. 5 Scanning electron microscopy images of expanded graphite obtained by chemical (CI) and electrochemical (EI) intercalation of natural flake graphite. Reproduced with permission [47]

on the roads [53]. Table 3 summarizes the price of imported flake graphite to the United States from 2009 to 2013 [18]. The cost of graphite has increased from \$694 per metric ton in 2009 to \$1360 per metric ton in 2013 (~100 % increased in the prices).

Accordingly, in order to meet future demand of graphite for battery production, recycling the waste sources of flake graphite should be considered for countries like the United States. In addition, considering the fact that NFG undergoes many upgrading processes and expenses to become qualified for LIB manufacturing, recycling used graphite anodes to the grade that could be reused in LIBs could be a key solution to these challenging issues.

4 Potential recycling sources

Flake graphite recycling has not been a major consideration in the past due to its abundance and favorable price. Apart from the battery industry, there are several other industries that use NFG as raw material. Therefore, their products could be considered as potential NFG recycling sources at the end of their life-time. Major applications of flake graphite are in the production of steel furnace refractories,

casting processes, crucibles, brake lining, and lubricants [19, 25, 54]. Table 4 specifies different applications of flake graphite.

Among these applications, steel furnace refractories are the consumers of almost 40 % of the NFG [21]. The waste that comes from steel making industry is known as “kish” and the graphite content of this waste is called kish graphite. A considerable tonnage of kish graphite is produced daily in steel production [55]. X-ray diffraction analysis has shown that the structure of kish graphite is almost identical to that of NG [56, 57]. Generally, industrial kish graphite exhibits a flake like appearance and the majority of the flakes are coarse size flakes [58]. The feasibility of recycling high quality flake graphite from kish has been investigated in the literature and reported to be successful in producing flake graphite with even improved crystallinity when compared to raw NFG [59, 60]. Therefore, kish recovered flake graphite could be a potential source of spherical graphite production for LIBs. Although the demand and future market growth of high quality NFG has been recognized since 1997, no commercial kish recovered flake graphite is available [18, 59]. Recycled flake graphite from other refractory industries goes to brake linings and thermal insulation production due to the lower level of quality [18].

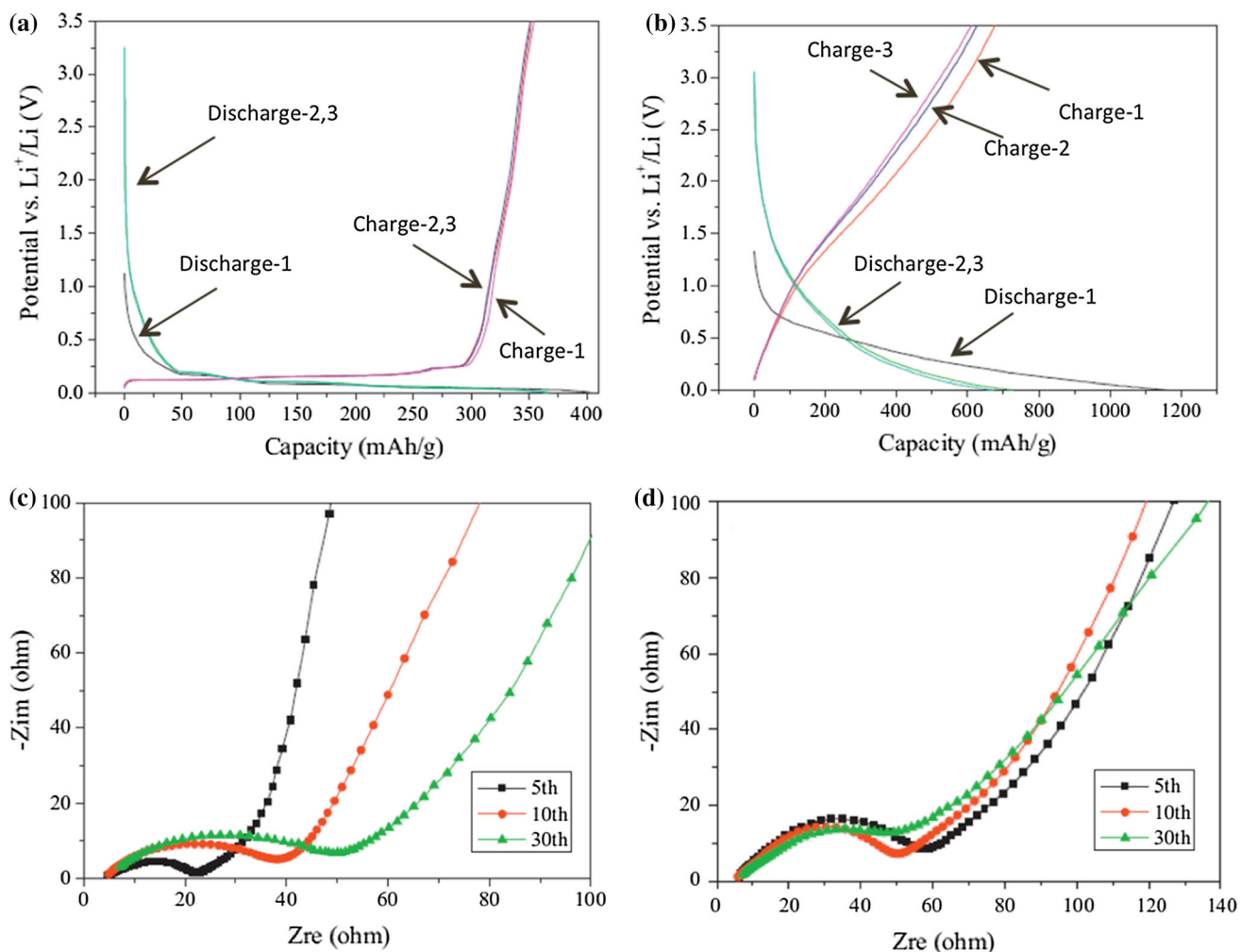


Fig. 6 First three discharge/charge curves of **a** natural flake graphite and **b** expanded graphite electrodes at a current density of 0.2 mA cm^{-2} . Altering current (AC) impedance spectra for the **c** natural graphite and **d** expanded graphite. Reproduced with permission [49]

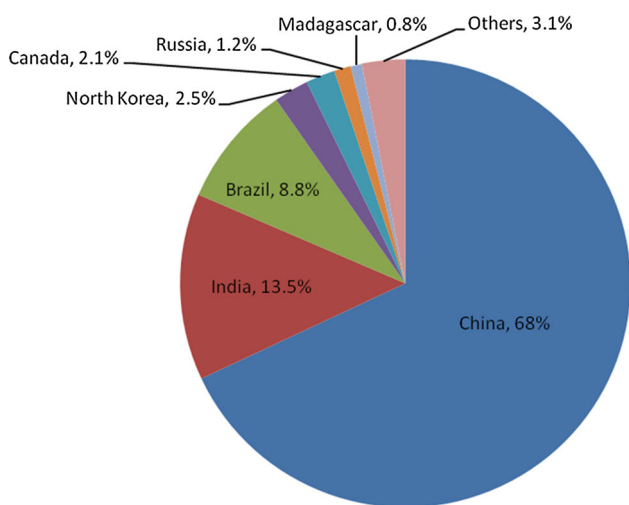


Fig. 7 The world natural graphite producing countries in 2013 [18]

Batteries, as one of the major consumers of flake graphite, could be considered a significant source for recycling battery grade materials. LIBs have been recycled using various methods from laboratory to successful commercial scale and the quality of the recycled products could vary from basic elements to battery-grade-materials [6, 9, 14, 61–67]. Most of these processes focus on recovery of lithium, cobalt, nickel, manganese, aluminum, and copper [38] in form of metallic alloys, compounds, or solutions containing metallic ions [9]. However, the carbon content of the batteries is either eliminated from the battery scrap by burning in furnaces or remains in after-filtration cakes as residue of the recycling process. The residue gets discarded or sent to steel-making industries.

Apart from flake graphite recycling, obtaining battery-grade carbon from various renewable and sustainable waste resources such as cherry stone, olive stone, mangrove

Table 3 Prices and import percentages of imported NFG to the United States [18]

Salient statistics—United States	2009	2010	2011	2012	2013
Price of imported flake graphite (average dollars per ton at foreign ports)	694	720	1180	1370	1360
Net import reliance as a percentage of apparent consumption	100	100	100	100	100

Table 4 Specification of graphite for different applications [25]

Application	Type	Carbon purity (%)	Flake size (μm)
Refractories			
Steel furnace refractories (magnesia graphite)	F	80–95	150–170
Casting processes (alumina graphite)	F	>85	50–500
Crucibles	A, F	80–90	>150
None-refractories			
Brake lining	A, F, V	>98	<75
Lubricants	A, F, V	98–99	53–106

Waste resources of steel furnace refractories and casting processes could be potential recycling resources of flake graphite. Reproduced with the permission of the British Geological Survey ©NERC. All rights Reserved

A amorphous, F flake, V vein

charcoal, rice husk, peanut shell, cotton wool, banana peels, and nonedible chicken egg-based waste have been reported in literature [68]. The recycled carbon from these resources structurally may belong to different types of graphitized or non-graphitized carbon. The carbon derived from the rice husk is in porous fibrous form showing superior electrochemical performance, especially in terms of rate performance (137 mAh g⁻¹ at 10C) [68]. The carbon synthesized from chicken egg is in the form of nitrogen-rich mesoporous carbon. This material exhibited a reversible capacity of 1780 mAh g⁻¹ as LIB anode, which is among the highest value achieved with carbon-based materials. Even the capacity at the 100th cycle (1365 mAh g⁻¹) has shown to be more than 3 times higher than the theoretical capacity of graphite (372 mAh g⁻¹) [69]. Anode material synthesized from waste banana peels (Banana peels pseudographite (BPPG)) has shown to work very well for LIBs, achieving 3 times the capacity of graphite. The graphite produced with this method has highly accessible near-surface nanopores for Li metal filling at low voltages and also substantial defect content in the graphene planes for Li adsorption at higher voltages [70].

Furthermore, non-renewable waste resources such as waste tires have been investigated for the production of functionalized carbon black. Recovery of such waste resources is beneficial for the recovery of carbon for LIBs as well as for controlling environmental hazards caused by waste tire stockpiles. The carbon recovered by this method has shown to have an ordered assembly of graphitic domains. Electrochemical studies revealed that this

material had a higher reversible capacity than that of graphite with a reversible capacity of 390 mAh g⁻¹ after 100 cycles [71].

5 Recycling processes

The quality of the recycled materials from waste resources of batteries can vary from basic elements to battery grade material. Based on the quality of the recycling end products, recycling processes for LIBs can be categorized into three main classes: (1) Pyrometallurgical recycling or thermal treatment process, (2) Hydrometallurgical recycling or chemical process, and (3) direct physical process.

5.1 Pyrometallurgical recycling or thermal treatment process

This type of recycling involves thermal treatment by smelting of battery components at elevated temperatures, from which only metals such as nickel, cobalt, lithium, and zinc are recovered. In this approach, the role of thermal treatment is to concentrate and liberate materials from current collectors followed by carbon electrodes elimination and other organic compounds. Carbon electrodes are either burned or served as reductant for some of the metals [6, 66, 72]. In pyrometallurgical recycling, LIBs may or may not undergo pre-separation of battery components before smelting. Therefore, graphite and other negative

electrode materials may be fed into smelting furnace along with positive electrode materials. This approach considers batteries as a source of raw materials and is only capable of recovering metals as elements. The recovered metal elements may subsequently be used in battery materials production or other chemical industries such as steel making companies [9, 66, 67].

Umicore Company located in Belgium has developed the VAL'EASTM process for recycling some sort of batteries including LIBs. This process is mainly based on pyrometallurgical methods. Battery scrap is introduced to ultra-high temperature smelters without any sort of pre-separation where organic materials (plastics, electrolyte, and solvent) are burnt and carbon electrodes are used as reducing agent for some of the metals. Figure 8 shows a schematic of the Umicore pyrometallurgical recycling process. The primary focus of the process is to recycle Ni and Co as $\text{Ni}(\text{OH})_2$ and LiCoO_2 , respectively; the latter of which can be used in manufacturing new LIBs. Umicore method has a limited application in the recycling of LIBs with LiMn_2O_4 chemistry because lithium ends up in the smelter slag. Umicore claims that using recycled Co reduces the production energy for LiCoO_2 by 70 %, which

would be a tremendous improvement. If there is a reduction of cobalt use in LIBs, the concomitant lower yields of Co in the recycling stream could make Umicore's processes uneconomical. Up to now, pyrometallurgical methods are not considered a suitable choice for recycling LIBs neither economically nor environmentally. Also other metals such as Cu, Fe, Zn are recovered as elements in this process while Li and Al end up in the recycling slag. In addition high value graphite anodes get lost [14, 61, 66, 67].

Accurec company—located in Germany—employs a mechanical pre-treatment process to remove plastic components, Al and Cu foils, and steel compounds before introducing the LIBs waste to the pyrometallurgical step. This process focuses on recovering Li, Mn, and Co in the form of lithium oxide, lithium chloride, and cobalt-manganese alloy by using a vacuum distillation furnace. There is no indication or emphasis on separating graphite electrodes in the pre-treatment step. Hence, one can hypothesize that graphite ends up in the slag as the residue of the recycling process [9, 73].

SNAM Company—located in France [9, 63, 74]—, XStrata Nickel International Company -located in Canada and Norway [14, 75]—, and INMETCO Incorporated—located in the United States [9, 76]—recycle LIBs as a part of their battery recycling programs via pyrometallurgical technologies. SNAM produces a cobaltiferous mixture called “MELCO” from recycling LIBs. XStrata is only interested in the recovery of Cu, Ni, and Co content of LIBs and INMETCO recycles Fe, Co, and Ni as alloy for stainless steel production. All other organic materials including carbon and graphite electrodes go to the slag or are burned as energy source or fed into the chamber as reducing agents in these processes [76].

Apart from commercial LIBs recycling, using thermal treatment has been investigated in laboratory scale in different stages of the recycling process. Lee and Rhee used a combined process for recycling spent LIBs shown in Fig. 9. By a two-step thermal treatment followed by shredding, and two screening steps, cathodic active materials were separated from other materials. All of the battery materials—including graphite—are introduced to the first thermal treatment furnace without pre-separation. It can be assumed that a part of the graphite anode has been separated as filtrate. The rest of the graphite and carbon content of the batteries that are not separated via screening are burned off by calcination at 500–900 °C [77]. Bahgat et al. [78] reported a process for recycling LIBs using the same route with minor modifications. They separated cathode and anode electrodes by means of shredder before the thermal treatment process. However, there is no information about recycling the separated graphite electrode in their process [78].

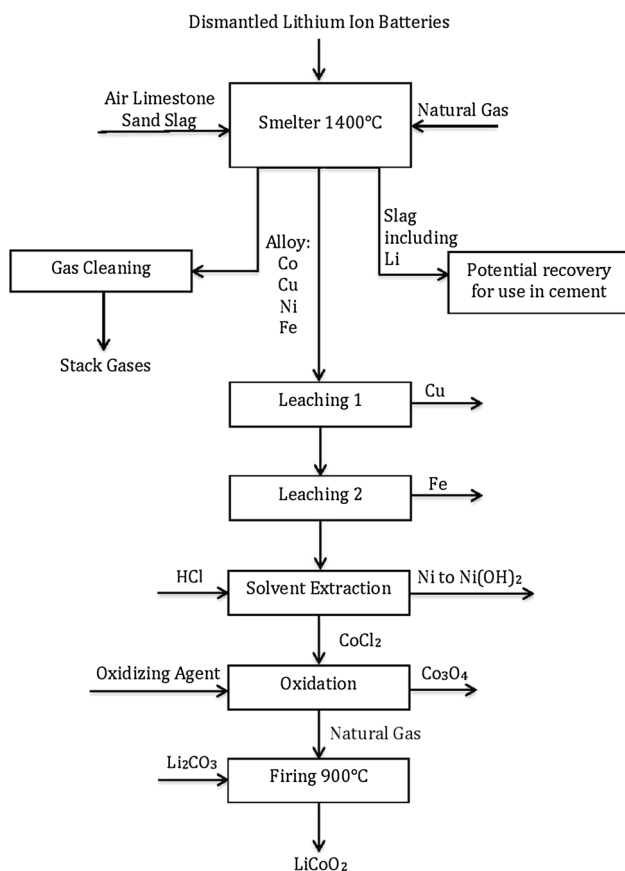


Fig. 8 Schematic of Umicore pyrometallurgical battery recycling process. Reproduced with permission [6]

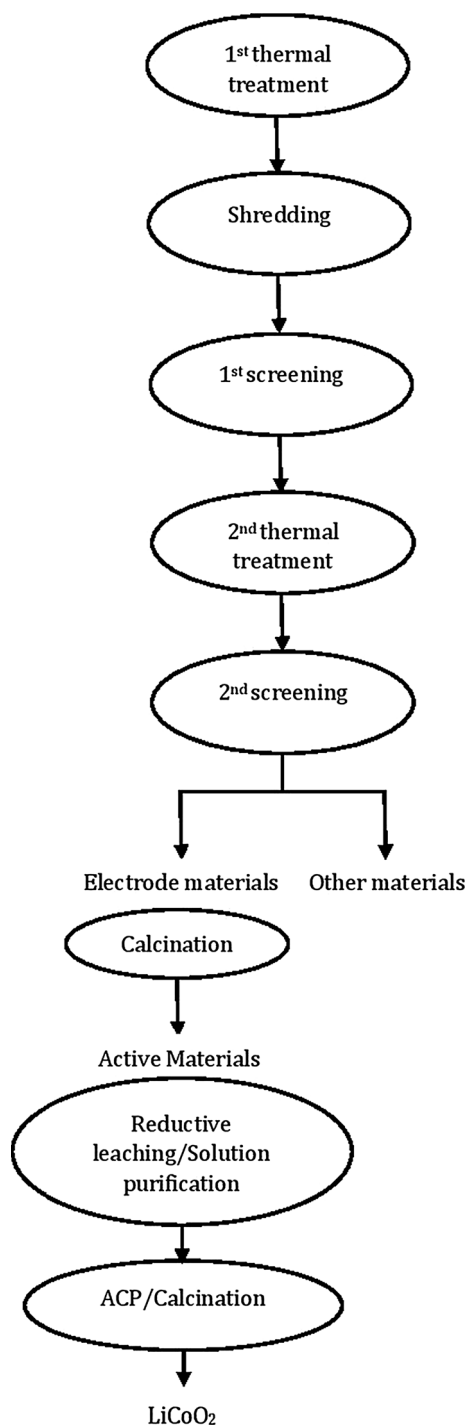


Fig. 9 Schematic of proposed recycling process for spent LIBs by Lee and Rhee. Reproduced with permission [77]

5.2 Hydrometallurgical recycling or chemical process

Hydrometallurgical processing technique consists of acid or base leaching for dissolving battery materials followed by purification processes such as chemical precipitation,

filtration, solvent extraction, and electrochemical processes. This method is capable of recovering almost all of the active materials. Negative electrode materials, including graphite, could potentially be recycled if the negative electrodes were separated from the positive electrodes by applying some types of mechanical separation processes before the leaching process [6, 63]. However, most of the pilot and commercial processes mainly aim on recovering electrolyte and valuable metals from the positive electrode, and even with the pre-mechanical separation steps only plastics, papers, iron, and copper sheets get separated and graphite goes to the leaching step and burns off by calcination [63, 67].

Most of the developed laboratory and commercial recycling processes for LIBs are hydrometallurgical based. Toxco Incorporated—located in Canada and the United States—has designed a series of low temperature mechanical and chemical procedures for recycling LIBs, shown in Fig. 10. The output of the mechanical separation process is three streams of materials, two of which contain valuable materials. The first stream is rich in Co, Cu, Ni, and Al. The second stream is called “Cobalt Filter Cake” which contains carbon mix, some cathode materials, and lithium carbonate. Lithium carbonate is separated from the second stream by adding soda ash. Currently, these two streams are sold for other products and there is no indication of graphite or carbon recovery from this process [61, 65–67, 79].

AEA Technology Batteries—located in the United Kingdom—has developed a set of mechanical, solvent extraction, and electrochemical processes for the recovery of LIBs. The electrolyte is recovered by extraction. Then, by dissolving the binder and filtration, lithium cobalt oxide and carbon mix are separated from current collectors, steel, and plastics. Eventually, electroreduction of lithium cobalt oxide separates lithium and cobalt from each other. The graphite present in the carbon mixture is left in the lithium cobalt oxide solution to increase the electronic conductivity for the electrochemical reduction of cobalt. There is no indication of graphite or carbon recovery from this process [79].

Recupyl’s process—a company located in Switzerland—involves mechanical and chemical treatment steps. Copper, aluminum, and steel can be recovered by mechanical treatment. Cobalt and lithium products are generated by chemical treatment [61, 80]. Similarly, Chemetall—company based in the United States—mostly targets recovering lithium in the form of LiOH by a series of leaching, solvent extraction, crystallization, ion exchange, and electro dialysis steps. Again, no graphite recovery step has been reported [61].

In summary, there are many hydrometallurgical-based LIB recycling research studies that have been performed

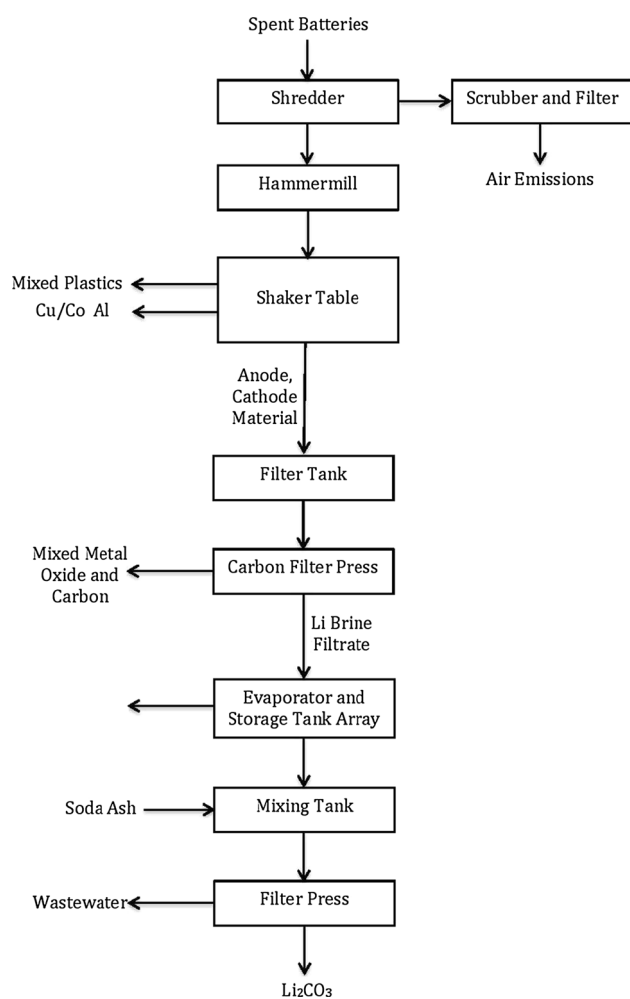


Fig. 10 A flow sheet of Toxco physical LIBs recycling process. Reproduced with permission [6]

from lab to the pilot scale, most of which aimed to recover metallic components of the LIBs. In the majority of these procedures, graphite and carbon contents are mostly separated by filtration as residue and at the best condition are suitable for re-use in lower quality applications not for high quality graphite recovery [13, 77, 81–84]. Figure 11 shows an overview of such recycling processes.

5.3 Direct physical recycling process

The direct physical process is designed for the recovery of battery grade materials for reusing in new LIBs production with little or no additional modification. The process involves multiple physical and chemical processes with a low temperature and energy requirement to separate battery components. This process can recover all active materials and metals, except the separator. In order to re-use the recovered materials in new batteries, extra purification or reactivating steps maybe necessary. Notably, this process is not commercialized yet [6, 67].

Eco-bat Technologies—housed in multiple countries in Europe—is mainly focused on recycling lead-acid batteries in a closed recycling loop, i.e. the recycled materials are used directly in new lead-acid batteries production [61, 66, 85]. Eco-bat has also developed a bench scale scheme for recycling valuable materials from LIBs as high quality battery grade materials. The process uses low-temperature units and consumes minimal energy. Figure 12 demonstrates this process for spent LIBs with LiCoO_2 as the cathode active material. By minimal disassembling of batteries' packages and using supercritical CO_2 , the electrolyte (ethyl methyl carbonate—EMC—, dimethyl carbonate—DMC—, LiPF_6) is extracted and then the remainder parts undergo pulverization or size-reduction steps. Subsequently, battery components are processed by a series of separation processes based on electronic conductivity and density differences using methods such as using a capacitor plate, a cyclone fluidized bed, and through solution dispersion coupled with decantation and filtration. Using this low-temperature process, electrolyte, metals parts, graphite anodes, and salts are recovered without taking them back to elements. The recycled graphite has the potential to be valuable as an anode material. These carbons have undergone lithium intercalation and have not been reintroduced to air or water in the recycling treatment program. Therefore, they have established pathways for lithium ion movement and their surfaces have been stripped of reactive functional groups. Only the separator is not recycled. The recycled components may undergo some treatment procedures before reinsertion into new batteries [66, 86]. The active-material structures are maintained, and the developers have demonstrated that new batteries can be produced from them with only minimal treatment. Over 80 % of the material is actually recycled to useful products. Thus, the potential value of the recovered materials is quite high. The cost of recovered cobalt is well below the current market price for virgin material. The authors reported a good cycle life performance of cells made with the recycled material. Experimental results show promise for both cobalt and phosphate cathodes. Recognizably, processing a mixed feed would require additional separation steps to yield high-quality final products. There is no obvious barrier to scaling up this process [66].

Due to the recent increasing demand and subsequent cost growth of battery grade graphite, more research studies have been dedicated to recycling graphite from LIBs. Recently, a new patent has been found in this regard. The authors claim that by means of this process pre-lithiated graphite is re-produced by recycling LIBs. Through this process, batteries are disassembled in a specific state of degradation and the unique route of the process allows tunable levels of pre-lithiation of the graphite. It has been stated that the recycled graphite has

Fig. 11 Hydrometallurgical process for recycling spent LIBs (the *dotted line* indicates that the organic phase is returned to the extraction step for reuse). *Asterick* The cases involve an external plastic and an internal metallic case. S:L is the ratio of solid (battery scrap) to leachant (HCl acid), O:A is the ratio of organic to aqueous phase. PC-88A is the commercial name for 2-ethylhexylphosphonic acid mono-2-ethylhexyl ester, which is used as the extractant agent for the solvent extraction process of the cathode materials. Reproduced with permission [81]

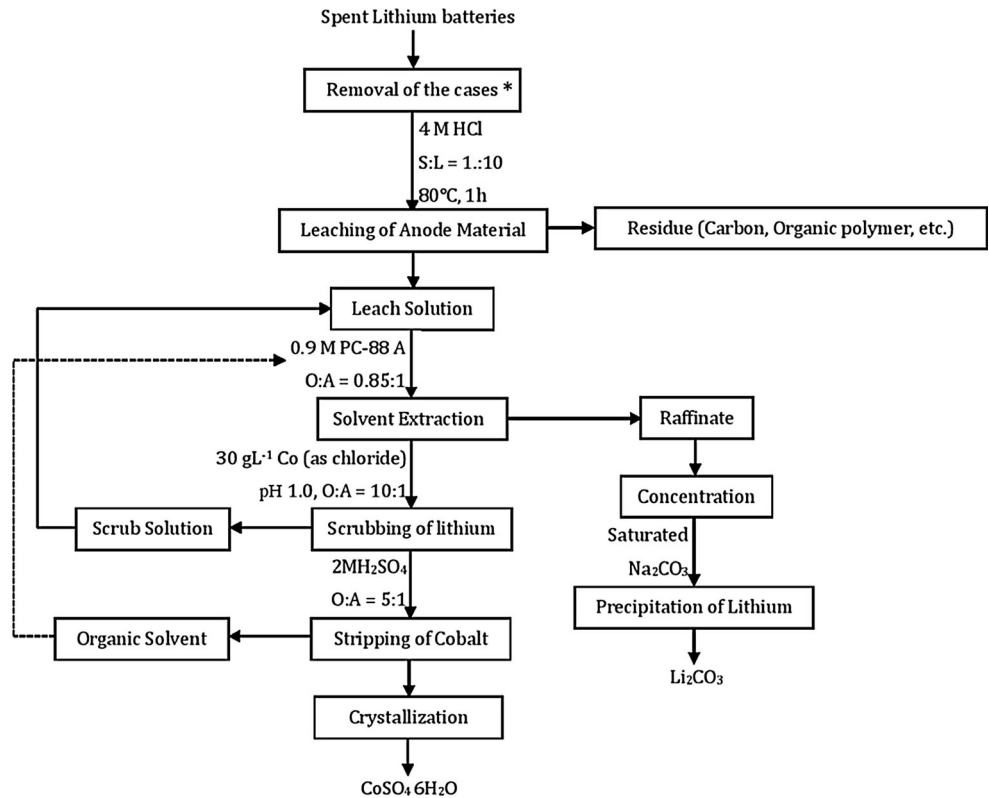
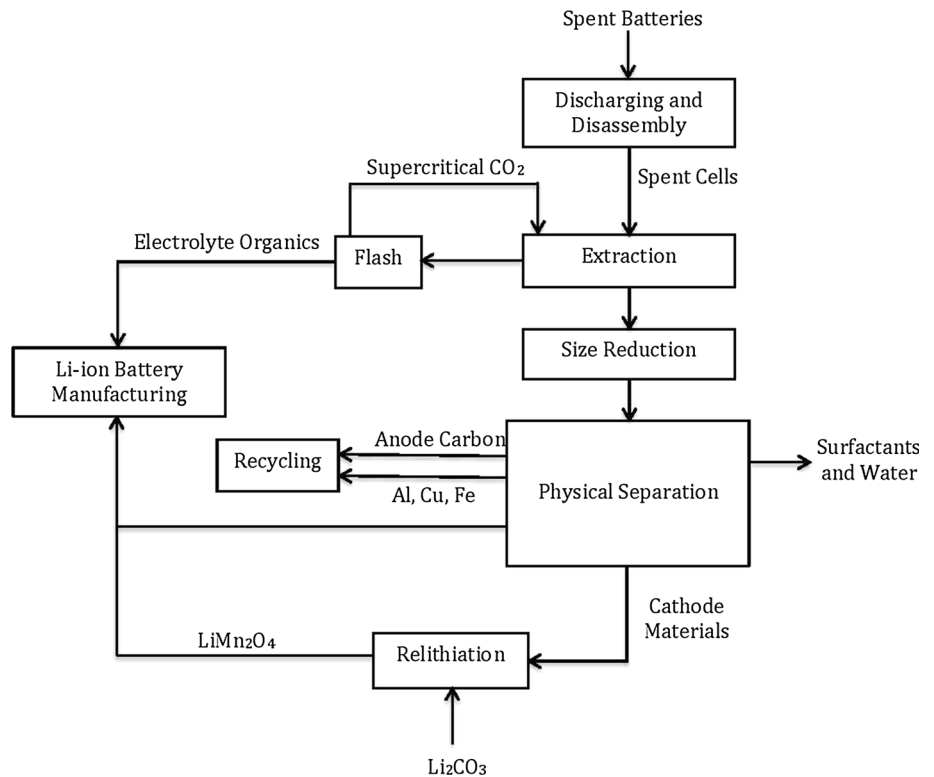


Fig. 12 Schematic of Eco-bat direct physical recycling process for LIBs with LiCoO_2 cathode. This process can recover all active materials and metals, except the separator. Reproduced with permission [6]



the proper quality for high energy/power applications [87].

Zhang et al. [88] compared impact of using wet versus dry crushing to minimize loss of valuable battery materials including graphite during recycling processes of spent LIBs used in mobile phones. Wet crushing involves using a blade crusher with water flow, which results in dissolution of fine graphite powder into water and loss of the active negative electrode material. Due to the water flow in wet crushing, the crushed anodes can quickly go through the mesh of the crusher. Therefore, the fine powder cannot be liberated from the copper foils in time, they all pass through the mesh together with water, which lead to an incomplete liberation; consequently, graphite does not stay on the mesh and is wasted, whereas using dry crushing, graphite electrode materials can be separated selectively from copper foil. However, screening fine particles is difficult by using dry screening; thus, there are finer particles in each fraction. Compared to dry screening, wet screening on wet crushed products provided a better screening effect in which particle sizes are homogeneous in each fraction. Comparing these two kinds of crushed products, it was manifested that fine particles of active electrode materials (LiCoO₂, graphite) in wet crushed products kept the original polymerization condition because of the presence of binder. Although in dry crushing more time was taken for electrode materials such as graphite and LiCoO₂ to liberate from copper foil and aluminous foil, dry method can bring selective crushing into full play. Electrode materials such as LiCoO₂ and graphite fully shed from aluminum foil and copper foil, then concentrate in fine fraction with less impurities and in loose structure, which created a favorable condition to subsequent recycling. This work demonstrates the potential of using dry crushing as one of the steps in future recycling processes, and in the case of the anode, recycling graphite [88].

Xiang et al. [89] studied the aging mechanism of graphite anodes by investigating a method for measuring specific capacity of graphite anodes in cycled LIBs. As a part of this research, they investigated recycling of graphite powder from cycled LIBs and re-using it in a new battery. The process proposed by the authors involves the following steps:

- (1) Disassembling the LIBs and taking out the graphite electrode plates followed by washing them with an organic solvent (e.g., DMC) to remove collected residue electrolyte from the surface of the electrode.
- (2) Drying of the plates for evaporation of the solvent. The drying temperature is preferably 85–100 °C.
- (3) Soaking the dried graphite electrode (from previous step) into HCl acid solution under ultrasonic vibration to separate the graphite film from the copper foil

and membrane completely. Moreover, the acidic solution step purifies graphite from the by-products of charge–discharge cycles, solid electrolyte interface layer, and carboxy methyl cellulose (CMC) thickener.

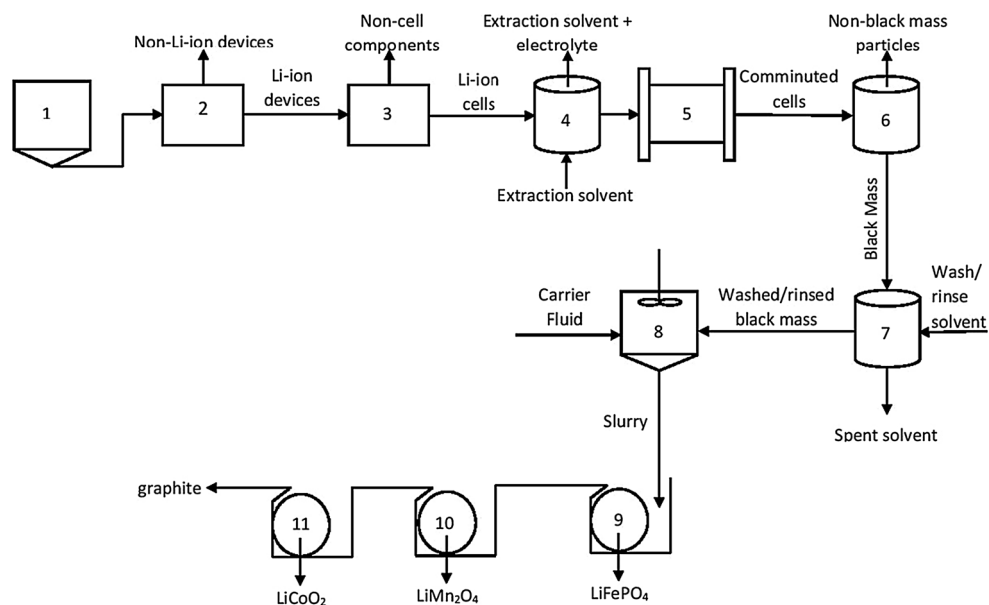
- (4) Separating the graphite powder from the acidic solution by centrifuging, rinsing, and drying.
- (5) Sieving, polishing, and preparing a negative electrode material from the dried powder to be inserted in a new battery.

Although, graphite anodes in real used batteries are aged and damaged in higher levels compared to cycled graphite of this study, the introduced method can be modified for recycling graphite anodes from used LIBs [89]. One of the challenges of this process is the recovery of the copper. An opportunity could be the integration of this process with electrowinning for the recovery of the copper dissolved in the acid [90–93]. Botte has proposed a new process -selective reduction electrowinning (SRE)- that allows the recovery of metals by using a sacrificial reductant such as ammonia and/or urea with significant advantages on the reduction of energy consumption when compared to classical electrowinning. Integration of the process proposed by Xiang et al. with electrowinning and SRE provides opportunities for the holistic recovery of the different parts of the battery [94].

Ellis and Montenegro [95] investigated a magnetic method for separating active electrode materials including graphite from electrochemical cells scrap containing used LIBs. Using multiple magnetic separators with different magnetic intensities, lithium metal compounds and nickel-containing compounds were separated. Graphite was recovered as non-magnetic fraction of the scrap. Afterwards, using magnetic separators with higher magnetic field intensity or field gradient, one electro active material was separated from other components. Figure 13 illustrates the cell recycle process and system using a staged magnetic separation of electrode active materials by increasing magnetic field intensities. The steps involved in the process include:

- (1) Collection of cell devices
- (2) Sorting to lithium-ion and non-lithium-ion devices (e.g., devices comprising lead-acid and nickel metal hydride chemistries)
- (3) Disassembly of LIBs into cells and non-cell components
- (4) Solvent extraction with an extraction solvent, such as supercritical CO₂
- (5) Commuting operation into particles using one or more of a knife mill, slitter mill, ball mill, pebble mill
- (6) Classification operation which separates anode and cathode materials into a black mass comprising

Fig. 13 Cell recycle process using a staged magnetic separation of electrode active materials by increasing magnetic field intensities. Reproduced with permission [95]



graphite, LiFePO_4 , LiMn_2O_4 , and LiCoO_2 using one or more sieving/screening unit operations

- (7) Washing and/or rinsing of black mass
- (8) Mixing black mass with a carrier fluid to produce a slurry containing a mixture of graphite, LiFePO_4 , LiMn_2O_4 , and LiCoO_2
- (9) Stage 1: Drum separator to recover the most magnetically susceptible material LiFePO_4
- (10) Stage 2: Drum separator to recover the second magnetically susceptible material LiMn_2O_4
- (11) Stage 3: Drum separator to recover the third magnetically susceptible material LiCoO_2 and the non-magnetic graphite in a non-magnetic fraction

In this specific process, graphite was separated in the last stage by applying a magnetic field. This process may produce highly pure electrode active metallic components and graphite with unaffected particle sizes and crystallography during the separation process. This environmentally friendly process may allow direct-reuse of the recycled metallic components without further chemical and thermal treatments. [95]. Recycled graphite may need to get more purified to be used again in new LIB cells. However, special attention should be focused on the recovery of the solvents used for washing and treating the black mass in the step 7 and/or the economic cost that this adds into the process. In step 7, the black mass may be treated with a wash solvent to dissolve and remove polymeric electrode binder from the electrode active materials. Suitable wash solvents introduced in the patent are *N*-methyl-2-pyrrolidone, tetrahydrofuran, ethanol, dimethyl carbonate, diethyl carbonate, dimethyl acetamide, diethyl formamide, methyl isobutyl ketone, and combinations of any thereof.

All of the mentioned solvents are considered hazardous waste. For instance, several studies have been performed on the recovery of *N*-methyl-2-pyrrolidone in LIBs production because it is a volatile and toxic organic solvent and is difficult to dispose [96–101]. Adding solvent recovery units to the whole recycling system may or may not justify the economical feasibility of this process.

In conclusion, pyrometallurgical and hydrometallurgical recycling processes mainly recover electrode active materials as elements or alloys. The materials recovered through these processes do not keep their structural and chemical form as they are in the original batteries. Therefore, more energy consumption and additional financial costs are needed to upgrade the recycled materials for re-using in the production of new cells. In contrary, direct recycling processes may offer promising results in recovering anode and cathode active materials from used LIBs in the structural and chemical forms present in the original cells. Consequently, recycled material may be directly re-used in new LIBs manufacturing. Table 5 summarizes major characteristics and graphite recycling status of the different LIBs recycling processes reviewed.

6 Challenges in recycling battery-grade graphite from spent LIBs

6.1 Economical justification

In the previous sections, the predicted increasing cost of the NFG was introduced as the main economical motivation for recycling reusable NFG from used LIBs. Furthermore, the potential strategies for recycling NFG from used

Table 5 Classification, characteristics, and status of graphite recycling processes for LIBs

Recycling process	Pyrometallurgical	Hydrometallurgical	Direct physical
Temperature	High	Low	Low
Materials recovered	Ni, Co, Li, Mn, Fe, Zn in alloy	Metal salts, Li ₂ CO ₃ or LiOH	Cathode, anode, electrolyte, metals
Graphite recycling status	Used as reducing agent or burned as energy source	Graphite can be separated if pre-mechanical separation is applied	Recovers potentially high-quality graphite

Recycling of graphite anodes could be potentially feasible via hydrometallurgical and direct physical recycling processes

LIBs have been discussed. However, from an economical standpoint, the competitive advantage of recycling NFG will depend on the cost of the recycling process, the market price of the battery-grade NFG, as well as the cost of disposing the NFG in used LIBs. For instance, Ellis and Montenegro's direct-recycling method that was described in a previous section involves the use of significant quantities of hazardous solvents [95]. Nowadays, regulations and laws pertaining to the recycling and disposal of hazardous waste are becoming stricter [102]. Solvent recovery and multiple unit operations associated with separation of components would increase the cost of the recycling process. Therefore, meeting the cost target in recycled NFG from LIBs may become one of the main challenges in recycling NFG from used LIBs.

6.2 Purity

Another important and challenging aspect associated with use of recycled graphite in LIBs is purity. As mentioned in previous sections, the purity of battery-grade graphite is 99.9 %. Therefore, the recycled graphite should be purified to the same level for reuse in the preparation of new electrodes. In preparation of graphite electrodes, NFG is mixed with a kind of polymeric binder (usually polyvinylidene fluoride) and possibly a type of carbon as an additive for conductivity improvement. Moreover, the electrode is in touch with the electrolyte and during the battery usage, the depositions from the electrolyte on the surface and into the structure of the electrode affects the purity of graphite. Consequently, removing all of the mentioned materials from graphite and achieving high purity recycled graphite may become challenging. Additional pre and/or post-treatment steps may become necessary to achieve the desired purity and thus the economical justification of recycling graphite gets affected.

6.3 Aging mechanism

Graphite anodes undergo various aging mechanisms, two of which prohibit re-using the recycled graphite in manufacturing new LIBs. These aging mechanisms affect the microstructure, crystallinity, and morphology of graphite

causing a decay of its electrochemical performance. The first aging mechanism is the graphite surface destruction and capacity loss during the first lithium intercalation/deintercalation cycle due to the formation of the solid-electrolyte-interface (SEI) film. The second mechanism is associated with the exfoliation and destruction of the graphite structure due to the co-intercalation of solvated lithium ions through the SEI film into the graphite layers [103].

Natural SEI film forms as a result of the irreversible reduction of the electrolyte at the electrode's surface during the first charging cycles of the cells. Two major reactions take place during the formation of the SEI: (1) chemical or electrochemical reaction of solvent and/or salt on the graphite surface (2) electrochemical reduction of the solvent molecules between graphene layers through a solvent co-intercalation with solvent ions [104]. At the SEI formation stage, lithium ions are consumed in the irreversible reaction. As SEI formation continues, not only more Li⁺ ions are consumed, but also the thickness of the film increases. The increased thickness of the passive SEI layer imbeds Li⁺ transfer. Therefore, the Li⁺ ions must tunnel through the layer. This mechanism results in the degradation of the graphite structure in fully charged batteries at storage conditions [105–108]. Moreover, formation of the SEI film is responsible for the irreversible capacity loss of graphite anodes. The theoretical capacity of graphite is 372 mAh g⁻¹, while its reversible capacity is only 251 mAh g⁻¹ (coulombic efficiency of 64 %) in the first cycle and its capacity fades to 105 mAh g⁻¹ in the first 10 cycles [109]. Ideally, the SEI film should be stable because unstable SEI film facilitates co-intercalation of solvated lithium ions and other solvent molecules. However, the SEI layer has an inhomogeneous and brittle nature [110]. Through the insertion and de-insertion of the big solvated molecules, graphite particles crack and split, which results in pulverization and exfoliation of crystalline graphite. Botte developed a mathematical model (VCP) that predicts significant changes in the radius of a single carbon fiber due to lithium intercalation/deintercalation when kinetics limitations are important, that is, at small particle size and low scan rates. Since LIBs are usually designed to operate under kinetics limitations (e.g., small particle size) volume

changes may play a significant role when predicting their performance. Based on this model the radius of a carbon fiber particle with initial radius of 1 μm can increase up to 7 % during lithium intercalation [111]. Combining a VCP model with particle size, porosity, and density distribution along with dimensions of the electrode, one can calculate the expansion of an electrode during lithium intercalation and this may be the key to understanding and predicting capacity fade during the cycling of LIBs. For instance, assuming the same increase in the radius of spherical graphite particles predicted by carbon fiber VCP model during lithium intercalation in an electrode and considering homogenous particle size distributed evenly (constant porosity) in a simple cubic structure and also assuming the particles are rigid bodies and neglecting interaction of the particles with binder, the volume of the electrode can change up to 21 %. Assuming rigid boundaries for the electrode inside of the battery package and a partial expansion accommodation by the void area available within the electrode, the expansion of the electrode causes cracks within the structure of the electrode. Figure 14 shows surface cracks on the graphite electrode from degradation. Although aging mechanisms do not normally change the crystal structure of graphite, they certainly make these particles less oriented, change the rhombohedral/hexagonal content during battery operation, and decrease the size of the original platelets [112–115].

In spite of the unfavorable outcomes of the SEI, its formation on the anode's surface is still necessary for maintaining electrode's stability and a smooth intercalation and deintercalation of lithium, since this film prevents the direct contact of graphite's surface and electrolyte [116,

117]. It also lets lithium ions move from the electrolyte solution into the carbon matrix due to its porous nature [2].

Overall, to benefit from the positive impact of SEI film on the performance of the anode and to minimize its adverse effects, numerous research studies have focused on the suppression of the irreversible capacity loss and prevention of the degradation of graphite by (1) proper choice of electrolyte components and electrolyte additives. Additives improve battery performance in several ways such as: facilitating formation of SEI on the surface of graphite, reduction of irreversible capacity and gas generation for the SEI formation and long-term cycling, and improving physical properties of the electrolyte such as conductivity and thus, decreasing electrolyte decomposition and SEI thickening, [118–124], and (2) surface modification of graphite by chemical, and electrochemical methods. The purpose of surface modification is to cover or modify graphite surface defects or edge sites where solvent decomposition mostly occurs [110, 125–128]. This method will be fully discussed in the next section.

Graphite's surface properties have a significant effect on the SEI formation, structural stability of the electrode, and the resulting electrochemical performance [129–134]. Therefore, among the different methods introduced above, surface modification is of great interest. Upon surface modification, the direct contact of graphite with the electrolyte solution is prevented; thus the decomposition of the electrolyte on the surface of graphite, the co-intercalation of the solvated lithium ions, and the charge-transfer resistance are decreased [2, 135]. All of these effects contribute to minimize irreversible capacity loss and deformation of graphite layers. Consequently, upon protecting graphite's surface and structure from degradation, the quality of the cycled graphite is expected to enhance and this will increase the potential for graphite recycling. Latest progress in research on surface modification methods adopted to mitigate these aging mechanisms in graphite anodes is described in the next section.

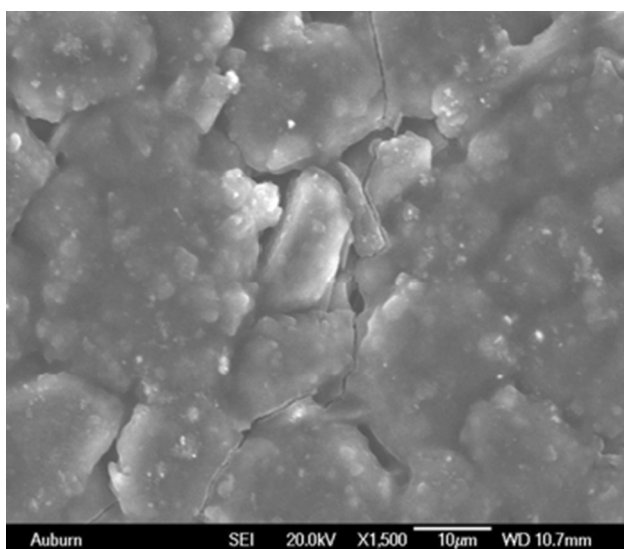


Fig. 14 Surface cracks on the surface of an aged anode electrode. Reproduced with permission [103]

7 Potential solutions to aging mechanisms in graphite anodes

7.1 Surface modification of graphite anodes

Previous studies have investigated various methods of surface modification of graphite electrodes such as mild oxidation [136–139], deposition of metals, metal oxides [135, 140–152], metal phosphate [153], coating with polymers [154–156], and other kinds of carbons [104, 157, 158]. Depending on the modification method, the following advantages could be achieved: (1) smoothing the active edge surfaces by removing some reactive sites and/or

defects on the graphite surface (2) forming a dense oxide layer on the graphite surface (3) covering active edge structures on the graphite surface, (4) creating nanochannels/micropores, (5) increasing the electronic conductivity, (6) reducing the thickness of the SEI layer, and (7) inhibiting structural changes during cycling. Among all of the mentioned methods of surface modification, deposition of certain metals or metal oxides which are hosts for lithium, provides an additional advantage: an increase in the number of host sites for lithium storage and improvement of the capacity of the anode. Therefore, surface modification of graphite by deposition of metals and metal oxides has been widely applied using different materials [2, 152]. Considering the importance of graphite recycling, the material to be deposited on the graphite surface and the deposition method should be in a way to prevent graphite recycling from becoming more challenging as it is, if not helping it. In the next section, recent developments in surface modification by deposition of metals and metal oxides on graphite anodes are reviewed.

7.2 Surface modification by deposition of metals and metal oxides

Surface coating by different metal and metal oxides such as Ni [139, 140], Sn [142–144], Zn [142], Ag [142, 145, 146], Al [147], Cu [148], Au [149], SnO [144], SnO₂ [150], Al₂O₃ [152], TiO₂ [135], and CuO, NiO, FeO, PbO [151] have been investigated in the literature.

Sn and SnO_x coated graphite powders showed higher coulombic efficiency, better rate capability, and longer cycle life. Also, Sn is a host of Li⁺, thus the capacity of the electrode improved as well [142–144, 150]. However, Sn has its own SEI layer and irreversible capacity loss in the first cycle. Veeraraghavan et al. [143] embedded Sn particles on the host graphite powder surface by using an electrocatalytic process. The substrates were pretreated in a reducing hypophosphite bath. Tin coating was carried out from an alkaline bath containing SnCl₂. Sodium hypophosphite was used as the reducing agent and sodium citrate served as the complexing agent for the autocatalytic reduction process [143]. When the surfaces of mesocarbon microbeads (MCMB) SG were coated with tin SnO₂, the reversible capacity was enhanced. However, the capacity of the coated MCMB fades with cycling due to the severe volume change of tin oxide from lithium cycling [150].

Yu et al. [140] used a novel encapsulation deposition technique for coating graphite powder with Ni composite at 85–90 °C in a plating bath containing sodium hypophosphite as a reducing agent. The coating consisted of Ni nanosized particles distributed over the surface of the graphite particle. Coating graphite's surface by nanosized Ni covered the surface of the graphite powders. Moreover,

the contact of the edge planes and the electrolyte solution was effectively prevented. The Ni coating prevents co-intercalation of solvated lithium ions and inhibits diffusion of solvent molecules into the graphite matrix. Additionally, subsequent reduction of PC and exfoliation of the graphene layers are greatly minimized. As a result, the cycling performance of the anode is improved [140]. In addition, due to the high conductivity of the Ni coating, exchange current densities and diffusion coefficients of the lithium ions were increased, whereas charge-transfer resistance and the surface film resistance were decreased in comparison to bare graphite. Furthermore, the composite exhibited less capacity loss over a 10-day storage period [139]. However, the capacity of the graphite was not improved since Ni is not a host for lithium.

In all of the previous studies, the coating was applied to graphite powder. In these methods, the electric conductivity of the electrode is restricted since the thickness and uniformity of the coating materials cannot be precisely controlled. So, the electric conduction pathway between the active and the coating materials was not well established to reinforce the electron transfer.

To address this issue, Jung et al. [152] reported an atomic layer deposition (ALD) method to apply a thin layer of Al₂O₃ coating on a graphite electrode. ALD is an advanced technology for applying ultrathin and homogeneous films on high-surface samples. The authors demonstrated that applying a conformal coating directly on the electrode (graphite + copper + binder) is critical to achieve optimal electrochemical performance for advanced LIBs. Figure 15a shows the transmission electron microscopy (TEM) image of the ALD Al₂O₃ coated MCMB with the thickness of 10 cycles of ALD reaction. Al₂O₃ coated graphite electrode demonstrated an improvement in cycle-ability compared to Al₂O₃ coated graphite powder. Bare NG displayed a relatively rapid decay in reversible capacity attributed to the instability of a SEI layer whereas the capacity retention was dramatically improved by Al₂O₃ ALD directly on the electrode [135]. However, a large irreversible reaction was observed, which resulted in lower full cell capacity because Al₂O₃ does not provide intercalation and extraction functions. Therefore, Al₂O₃ can only be used as a stabilizer to improve mechanical properties of graphite and to prevent excessive electrochemical reactions on the surface [152].

Wang and Wang studied the performance of an artificial SEI film of nanosized TiO₂ coated on graphite using ALD method. Figure 15b shows the TEM image of the ALD TiO₂ coated MCMB with the thickness of 10 cycles of ALD reaction. The batteries that used the ALD-TiO₂-coated graphite showed excellent cycle retention at elevated temperature, and the discharge capacity was substantially enhanced. TiO₂ coating increased graphite

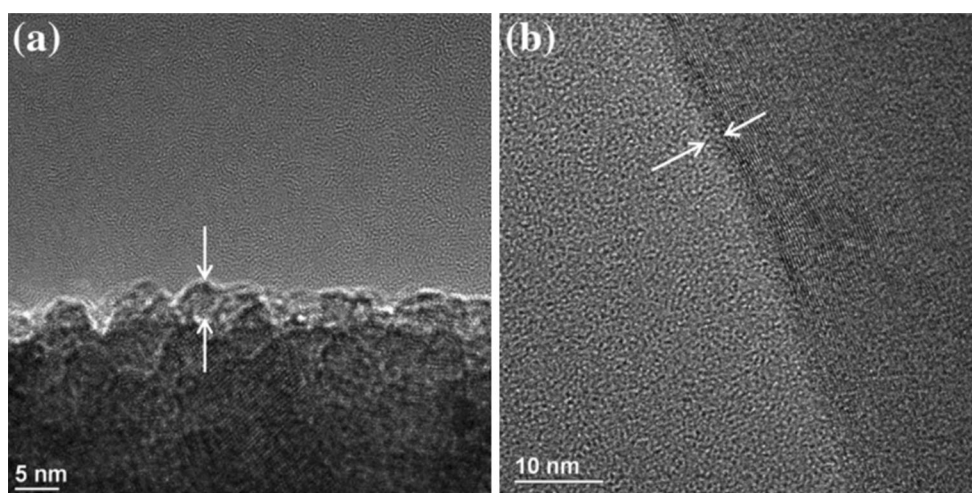


Fig. 15 Transmission electron microscopy images of **a** ALD Al_2O_3 coated mesocarbon microbeads and **b** ALD TiO_2 coated mesocarbon microbeads with the thickness of 10 cycles of ALD reaction. Reproduced with permission [135]

capacity by 5 % and constrained the formation of SEIs. In addition, the TiO_2 -coating improved thermal stability and greatly enhanced long-term cycle ability of the electrode at 55 °C [135].

7.3 Opportunities and new directions

Among transition metal oxides to be used for surface modification of graphite anodes, Fe_3O_4 shows high capacity (926 mAh g^{-1}), low cost, environmental benignity, and natural abundance. Furthermore, Fe_3O_4 shows relatively high electronic conductivity [159–161], thus has attracted considerable attention as an electrode material [161–170]. Besides, the highly magnetic behavior of Fe_3O_4 may play a significant role in recycling graphite from used surface modified graphite anodes.

However, Fe_3O_4 as anode material for LIBs shows poor capacity retention and fast capacity fading. The degradation in the performance of Fe_3O_4 anodes is attributed to the drastic volume change resulting in severe pulverization of the particles and loss of electrical connectivity upon electrochemical cycling. In addition, the formation of a thick SEI film on Fe_3O_4 anode surface causes a large initial irreversible capacity [162, 171].

One approach to minimize these issues is to synthesize nanostructure materials such as nanospindle, nanoparticles, nanosheets, nanowires, nanorods, nanotubes, and hollow nanostructures [162, 168–170, 172, 173]. The use of nanostructured materials improves the conductivity and charge/discharge rates because the path lengths for the transport of electrons and lithium ions in nanostructures are shorter than bulk materials. Moreover, these nanomaterials can accommodate the mechanical strain of lithium ion insertion/extraction much better than of micrometer-scale

materials [174–177]. However, using nanostructured transition metal oxides as anode materials increases the possibilities of side reactions involving electrolyte decomposition on electrodes surface because nanostructured materials have high surface area causing a high level of irreversibility, poor life cycle, and the formation of thick SEI films on the electrode surface, which consume much of the lithium ions [178].

Carbon coating is one of the most widely used surface modification techniques to solve the above problem for nanostructure transition metal oxides. Carbon materials are very stable in LIBs environment due to the small volume change during Li insertion/extraction. Furthermore, carbon-coating layers can significantly enhance the electronic conductivity, which results in improved rate performance [162, 179–181]. Also, The SEI films on carbon surface are also relatively stable [182–184]. For instance, carbon-coated Fe_3O_4 nanospindles [162], carbon-decorated single-crystalline Fe_3O_4 nanowires [163], Fe_3O_4 -based Cu nanoarchitecture [161], Fe_3O_4 /carbon core-shell nanorods [164], Fe_3O_4 -based nanotube arrays [165], graphene-wrapped Fe_3O_4 [171], and carbon-encapsulated Fe_3O_4 nanoparticles [174] have been used to improve the electrochemical performance of Fe_3O_4 electrodes.

Accordingly, carbon coated Fe_3O_4 nanoparticles deposited on graphite anodes are expected to simulate as a SEI layer to protect the surface of the graphite from degradation, increase the capacity of the anode, and decrease irreversible capacity. In this way, only coated Fe_3O_4 nanospindles are in contact with electrolyte. Considering the improvements of the direct deposition of Al_2O_3 and Ti on composite graphite anodes instead of graphite powder [135, 152], by direct deposition of carbon coated Fe_3O_4 nanoparticles even more improvements are

expected. By using a direct deposition method, carbon coated Fe_3O_4 nanoparticles are only accumulated on the surface of the graphite anodes; thus, one may capitalize on this advantage to recover graphite during recycling. For example, a magnetic field similar to Ellis and Montenegro's recycling process [95] could be possible; therefore, the hypothesis here is that graphite can be recycled from used LIBs and reused in new batteries' production.

Although, recently discovered anode materials such as Fe_3O_4 are not ready for scale up, their superior properties may be used for improvement of commercial graphite anodes in the next generation of LIBs.

8 Conclusion

A classification of graphite was introduced since graphite occurs in a variety of forms and properties. NG can be one of the forms of amorphous, flake, and vein. Besides, as a part of classification of graphite, spherical, synthetic, and expanded graphite were also described. Among all types of NG, flake graphite was discussed extensively since it is the mere natural source of anode material for LIBs. The future demand of flake graphite as a component of LIBs for vehicular applications was discussed. Because of the high demand of NFG, countries such as the United States and European Union countries with no graphite production consider flake graphite as a critical material. Recycling battery grade graphite from spent LIBs was proposed as one of the effective approaches to meet the significant predicted demand of battery grade graphite. Current status of graphite recycling from spent LIBs in laboratory to commercial scale processes was reviewed. Industrial-scale processes for the recycling of the electrode active materials generally fall into two categories: pyrometallurgical processes and hydrometallurgical processes. Pyrometallurgical processes involve the high-temperature smelting of battery scraps to produce various alloys, metallic oxides, and flue gases. Hydrometallurgical processes usually employ aggressive chemicals such as strong acids and/or strong bases to dissolve metals, alloys, and/or inorganic metal compounds, such as metal oxides, and extract or leach the active battery materials from spent LIBs. Pyrometallurgical and hydrometallurgical recycling processes both fail to recover graphite and other electrode active materials in the structural and chemical forms present in the original electrochemical cells. To address this issue, direct physical recycling process was introduced. This process enables the separation of recyclable anode and cathode active materials from electrochemical cell scrap. Post-treatment methods could potentially be used to recycle graphite anodes in the structure and chemical forms present in the original electrochemical cells. Using direct physical recycling methods

may form recycled material concentrates that may be directly re-used in new LIBs manufacturing. Therefore, direct physical recycling may eliminate the need for pyrometallurgical and hydrometallurgical recycling processes or be used in combination with pyrometallurgical, hydrometallurgical, and other recycling processes to recover electrode active materials from spent LIBs to be re-used in new LIBs production. However, there are several challenges in recovering battery grade graphite from spent LIBs. Graphite electrodes undergo several aging mechanisms such as formation of solid electrolyte interface (SEI) and co-intercalation of solvent molecules into the structure of graphite. The aging mechanisms were reviewed extensively. As a result of these aging mechanisms, capacity of graphite degrades and structural changes occur within graphite electrodes. To minimize degradation of graphite, surface modification technique was introduced and reviewed. Moreover, the gap in literature in using surface modification for graphite electrodes was recognized. For the new generation of LIBs, surface modification with the goal of improving graphite electrode's capacities, decreasing graphite degradation and irreversible capacity, and minimizing graphite recycling challenges after the lifetime of the battery was recommended. An example of this new perspective in surface modification of graphite electrodes was also proposed as a future research opportunity in this area.

Acknowledgments Financial support from the Chemical and Biomolecular Engineering department and the Center for Electrochemical Research (CEER) at Ohio University is greatly appreciated.

References

1. De las Casas C, Li W (2012) A review of application of carbon nanotubes for lithium ion battery anode material. *J Power Sour* 208:74–85. doi:[10.1016/j.jpowsour.2012.02.013](https://doi.org/10.1016/j.jpowsour.2012.02.013)
2. Fu LJ, Liu H, Li C, Wu YP, Rahm E, Holze R, Wu HQ (2006) Surface modifications of electrode materials for lithium ion batteries. *Solid State Sci* 8(2):113–128. doi:[10.1016/j.solidstatesciences.2005.10.019](https://doi.org/10.1016/j.solidstatesciences.2005.10.019)
3. Etacheri V, Marom R, Elazari R, Salitra G, Aurbach D (2011) Challenges in the development of advanced Li-ion batteries: a review. *Energy Environ Sci* 4(9):3243–3262. doi:[10.1039/c1ee01598b](https://doi.org/10.1039/c1ee01598b)
4. Goonan TG (2012) Lithium use in batteries. U.S. Geological Survey, Reston
5. Kassatly SSN (2010) The lithium-ion battery industry for electric vehicles. Thesis, Massachusetts Institute of Technology, Boston
6. Dunn JB, Gaines L, Barnes M, Sullivan J and Wang M (2012) Material and energy flows in the materials production, assemble, and end-of-life stages of the automotive lithium-ion battery life cycle, Report ANL/ESD/12-3. Argonne National Laboratory (ANL) Argonne, IL
7. Gaines L and Nelson P (2010) Lithium-ion batteries: possible materials issues. In: 13th international battery materials

- recycling seminar and exhibit, Broward County Convention Center, Fort Lauderdale, Florida, March 16–18, 2009, p 16
8. Scrosati B, Garche J (2010) Lithium batteries: status, prospects and future. *J Power Sour* 195(9):2419–2430. doi:10.1016/j.jpowsour.2009.11.048
 9. Bernardes A, Espinosa DCR, Tenorio JS (2004) Recycling of batteries: a review of current processes and technologies. *J Power Sour* 130(1):291–298. doi:10.1016/j.jpowsour.2003.12.026
 10. Wu Q, Lu W, Prakash J (2000) Characterization of a commercial size cylindrical Li-ion cell with a reference electrode. *J Power Sour* 88(2):237–242. doi:10.1016/S0378-7753(00)00372-4
 11. Iwakura C, Fukumoto Y, Inoue H, Ohashi S, Kobayashi S, Tada H, Abe M (1997) Electrochemical characterization of various metal foils as a current collector of positive electrode for rechargeable lithium batteries. *J Power Sour* 68(2):301–303. doi:10.1016/S0378-7753(97)02538-X
 12. Chen J, Yao C, Sheu S, Chiou Y, Shih H (1997) The study of carbon half-cell voltage in lithium-ion secondary batteries. *J Power Sour* 68(2):242–244. doi:10.1016/S0378-7753(97)02650-5
 13. Shin SM, Kim NH, Sohn JS, Yang DH, Kim YH (2005) Development of a metal recovery process from Li-ion battery wastes. *Hydrometallurgy* 79(3):172–181. doi:10.1016/j.hydro.2005.06.004
 14. Georgi-Maschler T, Friedrich B, Weyhe R, Heegn H, Rutz M (2012) Development of a recycling process for Li-ion batteries. *J Power Sour* 207:173–182. doi:10.1016/j.jpowsour.2012.01.152
 15. Vayrynen A, Salminen J (2012) Lithium ion battery production. *J Chem Thermodyn* 46:80–85. doi:10.1016/j.jct.2011.09.005
 16. Bade R, Pidgeon N, Greene M (2012) Graphite, review sector, liberties. http://minesite.com/media/pub/var/release_downloadable_file/38247.pdf. Accessed April 2014
 17. Cobb J June 2014 dashboard. <http://www.hybridcars.com/june-2014-dashboard/>. Accessed July 2014
 18. Oslon DW (2014) Graphite (Natural). United States Geological Survey, Mineral commodity summaries
 19. Syrah Resources, Graphite Industry Report. (2012). http://www.investment-hr.com/next_opper_doc/Graphite.industry.Report.pdf. Accessed May 2014
 20. Tesla battery plant will need 6 new flake graphite mines (2014) Industrial minerals. <http://www.indmin.com/Article/3315690/Tesla-battery-plant-will-need-6-new-flake-graphite-mines.html>. Accessed April 2014
 21. Graphite Industry and Balama Marketing Update (2013) Syrah Resources Ltd. http://hotcopper.com.au/threads/ann-graphite-industry-and-balama-marketing-updat.2008347/-U_4_K2NiJQo. Accessed April 2014
 22. Concern over battery grade graphite supplies. (2010) Industrial mineral. <http://www.northerngraphite.com/wp-content/uploads/2010/08/Concern-over-battery-grade-graphite-supplies.pdf>. Accessed June 2014
 23. Guo P, Song H, Chen X (2009) Electrochemical performance of graphene nanosheets as anode material for lithium-ion batteries. *Electrochem Commun* 11(6):1320–1324. doi:10.1016/j.elecom.2009.04.036
 24. Weis PL (1973) United States Mineral Resources. Geological Survey Professional Paper, vol 820
 25. Mitchell C (1992) Industrial Minerals Laboratory Manual: Flake graphite, Technical Report WG/92/30 British Geological Survey
 26. Wissler M (2006) Graphite and carbon powders for electrochemical applications. *J Power Sour* 156(2):142–150. doi:10.1016/j.jpowsour.2006.02.064
 27. Dissanayake CB (1981) The origin of graphite of Sri Lanka. *Org Geochem* 3(1–2):1–7. doi:10.1016/0146-6380(81)90006-1
 28. Taylor HA (2000) Graphite, natural. In: Kirk-othmer encyclopedia of chemical technology. Wiley, New York. doi:10.1002/0471238961.1401202120012512.a01
 29. Mukhopadhyay P, Gupta RK (2012) Graphite, graphene, and their polymer nanocomposites. CRC Press, Boca Raton
 30. Ohzeki K, Saito Y, Golman B, Shinohara K (2005) Shape modification of graphite particles by rotational impact blending. *Carbon* 43(8):1673–1679. doi:10.1016/j.carbon.2005.02.007
 31. Zaghbi K, Song X, Guerfi A, Rioux R, Kinoshita K (2003) Purification process of natural graphite as anode for Li-ion batteries: chemical versus thermal. *J Power Sour* 119–121:8–15. doi:10.1016/S0378-7753(03)00116-2
 32. Markel RF, Goldberger W (1979) Method for heat treating carbonaceous material in a fluidized bed. United States Patent US4160813 A, July 10, 1979
 33. Takahashi M, Ohshita R, Ueno K, Nishio K, Saitoh T (1994) Lithium secondary batteries. European Patent EP0624913 A2, March 30, 1993
 34. Yoshio M, Wang H, Fukuda K (2003) Spherical carbon-coated natural graphite as a lithium-ion battery-anode material. *Angew Chem* 115(35):4335–4338. doi:10.1002/ange.200351203
 35. Yoshio M, Wang H, Fukuda K, Umeno T, Abe T, Ogumi Z (2004) Improvement of natural graphite as a lithium-ion battery anode material, from raw flake to carbon-coated sphere. *J Mater Chem* 14(11):1754–1758. doi:10.1039/B316702J
 36. Wang X, Gai G-S, Yang Y-F, Shen W-C (2008) Preparation of natural microcrystalline graphite with high sphericity and narrow size distribution. *Powder Technol* 181(1):51–56. doi:10.1016/j.powtec.2007.06.025
 37. Chen G, Fang Q, Jang BZ, Shi J, Wang MC, Zhamu A (2010) Graphite or carbon particulates for the lithium ion battery anode. United States Patent US20120021294 A1, Jan 26, 2012
 38. Juri G, Wilhelm HA, L'Heureux J High Purity Graphite Powders for High Performance. Timcal Graphite and Carbon. [http://www.timcal.ch/Scopi/Group/Timcal/timcal.nsf/pagesref/MCOA-7S6H6L/\\$File/High_purity_graphite_powders_for_high_performance.pdf](http://www.timcal.ch/Scopi/Group/Timcal/timcal.nsf/pagesref/MCOA-7S6H6L/$File/High_purity_graphite_powders_for_high_performance.pdf). Accessed Feb 2014
 39. Feytis A (2010) The bright side of graphite. <http://www.northerngraphite.com/wp-content/uploads/2010/08/Graphite-feature-july-2010.pdf>. Accessed May 2014
 40. Li J, Daniel C, Wood D (2011) Materials processing for lithium-ion batteries. *J Power Sour* 196(5):2452–2460. doi:10.1016/j.jpowsour.2010.11.001
 41. Markevich E, Baranchugov V, Salitra G, Aurbach D, Schmidt MA (2008) Behavior of graphite electrodes in solutions based on ionic liquids in in situ Raman studies. *J Electrochem Soc* 155(2):A132–A137. doi:10.1149/1.2811897
 42. Baranchugov V, Markevich E, Salitra G, Aurbach D, Semrau G, Schmidt MA (2008) In situ Raman spectroscopy study of different kinds of graphite electrodes in ionic liquid electrolytes. *J Electrochem Soc* 155(3):A217–A227. doi:10.1149/1.2828858
 43. Aurbach D, Teller H, Koltypin M, Levi E (2003) On the behavior of different types of graphite anodes. *J Power Sour* 119–121:2–7. doi:10.1016/S0378-7753(03)00115-0
 44. Lu M, Cheng H, Yang Y (2008) A comparison of solid electrolyte interphase (SEI) on the artificial graphite anode of the aged and cycled commercial lithium ion cells. *Electrochim Acta* 53(9):3539–3546. doi:10.1016/j.electacta.2007.09.062
 45. Report on Critical Raw Materials for the EU. European Commission. http://ec.europa.eu/enterprise/policies/raw-materials/documents/index_en.htm. Accessed June 2014
 46. Amaraweera T, Balasooriya N, Wijayasinghe H, Attanayake A, Dissanayake M (2013) Purity enhancement of Sri Lankan vein graphite for lithium-ion rechargeable battery anode. In: 29th Technical Sessions of Geological Society of Sri Lanka, p 104

47. Vieira F, Cisneros I, Sansiviero M, Miranda A, Rosa N, Lima U, Mohallem N (2006) Preparation processes and properties of expanded graphite for alkaline batteries. *J Phys Chem Solids* 67(5):1208–1212. doi:10.1016/j.jpcs.2006.01.050
48. Park D-Y, Lim Y-S, Kim M-S (2010) Performance of expanded graphite as anode materials for high power li-ion secondary batteries. *Carbon Lett* 11:343–346
49. Bai L-Z, Zhao D-L, Zhang T-M, Xie W-G, Zhang J-M, Shen Z-M (2013) A comparative study of electrochemical performance of graphene sheets, expanded graphite and natural graphite as anode materials for lithium-ion batteries. *Electrochim Acta* 107:555–561. doi:10.1016/j.electacta.2013.06.032
50. Lin Y, Huang Z-H, Yu X, Shen W, Zheng Y, Kang F (2014) Mildly expanded graphite for anode materials of lithium ion battery synthesized with perchloric acid. *Electrochim Acta* 116:170–174. doi:10.1016/j.electacta.2013.11.057
51. Shaw S (2013) Increasing demand for high purity natural graphite in new applications Roskill. <http://www.roskill.com/news/increasing-demand-for-high-purity-natural-graphite-in-new-applications>. Accessed May 2014
52. Risk List of 2012. (2012). <http://www.bgs.ac.uk/mineralsuk/statistics/risklist.html>. Accessed June 2014
53. Sikes K, Gross T, Lin Z, Sullivan J, Cleary T, Ward J (2010) Plug-in hybrid electric vehicle market introduction study: final report. <http://www.osti.gov/scitech/servlets/purl/972306/>. Accessed July 2014
54. Laverty PD, Nicks LJ and Walters LA (1994) Recovery of Flake Graphite From Steelmaking Kish, US Department of Interior, Bureau of Mines
55. Ubbelohde AR, Lewis FA (1960) Graphite and its crystal compounds. Clarendon Press, Oxford, London
56. Walker P, Imperial G (1957) Structure of graphites: graphitic character of kish. *Nature* 180:1185. doi:10.1038/1801185a0
57. Matuyama E (1959) Structure of kish and other graphites. *Nature* 183:670–671. doi:10.1038/183670b0
58. Liu S, Loper CR Jr (1991) The formation of kish graphite. *Carbon* 29(4):547–555. doi:10.1016/0008-6223(91)90119-4
59. Bennett GW, Leduc M, St-Hilaire JG, Garceau C (1997) Beneficiation of kish graphite. *Unites States Patent US5672327 A*, September 30
60. Nicks LJ, Nehl FH, Chambers MF (1995) Recovering flake graphite from steelmaking kish. *J Mineral, Metals Mater Soc* 47(6):48–51. doi:10.1007/bf03221205
61. Dunn J, Gaines L, Barnes M, Sullivan J Impacts of the Manufacturing and Recycling Stages on Battery Life Cycles. Argonne National Laboratory, Energy Systems Division, Department of Mechanical Engineering. <http://www.transportation.anl.gov/pdfs/B/836.PDF>. Accessed Jan 2014
62. Zackrisson M, Avellán L, Orlenius J (2011) Life cycle assessment of lithium-ion batteries for plug-in hybrid electric vehicles-critical issues. *J Clean Prod* 18(15):1519–1529. doi:10.1016/j.jclepro.2010.06.004
63. Xu J, Thomas H, Francis RW, Lum KR, Wang J, Liang B (2008) A review of processes and technologies for the recycling of lithium-ion secondary batteries. *J Power Sour* 177(2):512–527. doi:10.1016/j.jpowsour.2007.11.074
64. Granata G, Pagnanelli F, Moscardini E, Takacova Z, Havlik T, Toro L (2012) Simultaneous recycling of nickel metal hydride, lithium ion and primary lithium batteries: accomplishment of European guidelines by optimizing mechanical pre-treatment and solvent extraction operations. *J Power Sour* 212:205–211. doi:10.1016/j.jpowsour.2012.04.016
65. Sullivan J, Gaines L (2010) A review of battery life-cycle analysis: state of knowledge and critical needs, No. ANL/ESD/10-7. Argonne National Laboratory (ANL). <http://www.osti.gov/scitech/biblio/1000659>. Accessed May 2014
66. Gaines L, Sullivan J, Burnham A, Belharouak I Life-cycle analysis for lithium-ion battery production and recycling. In: Transportation Research Board 90th Annual Meeting Washington, DC, January 23–27, 2011
67. Sullivan J, Gaines L, Burnham A Role of recycling in the life cycle of batteries. In: TMS 2011 140th annual meeting and exhibition, materials processing and energy materials, 2011. Wiley, New York, p 25
68. Wang L, Schnepf Z, Titirici MM (2013) Rice husk-derived carbon anodes for lithium ion batteries. *J Mater Chem A* 1:5269. doi:10.1039/c3ta10650k
69. Li Z, Xu Z, Tan X, Wang H, Holt CMB, Stephenson T, Olsen BC, Mitlin D (2013) Mesoporous nitrogen-rich carbons derived from protein for ultra-high capacity battery anodes and supercapacitors. *Energy Environ Sci* 6:871–878. doi:10.1039/c2ee23599d
70. Memarzadeh Lotfabad E, Ding J, Cui K, Kohandehghan A, Kalisvaart WP, Hazelton M, Mitlin D (2014) High-density sodium and lithium ion battery anodes from banana peels. *ACS Nano* 8(7):7115–7129. doi:10.1021/nm502045y
71. Naskar AK, Bi Z, Li Y, Akato SK, Saha D, Chi M, Bridges CA, Paranthaman MP (2014) Tailored recovery of carbons from waste tires for enhanced performance as anodes in lithium-ion batteries. *RCS Adv* 4:38213. doi:10.1039/c4ra03888f
72. Castillo S, Ansart F, Laberty-Robert C, Portal J (2002) Advances in the recovering of spent lithium battery compounds. *J Power Sour* 112(1):247–254. doi:10.1016/S0378-7753(02)00361-0
73. <http://www.accurec.de/treatment-and-recycling/technologies/lion>. Accessed March 2014
74. <http://www.snam.com/activites/recycling-snam-next.php>. Accessed April 2014
75. Ellis TW, Mirza AH (2011) Battery recycling: defining the market and identifying the technology required to keep high value materials in the economy and out of the waste dump. National Institute of Standards and Technology (NIST), USA. http://www.nist.gov/tip/wp/pswp/upload/245_battery_recycling_defining_the_market.pdf. Accessed May 2014
76. Espinosa DCR, Bernardes AM, Tenório JAS (2004) An overview on the current processes for the recycling of batteries. *J Power Sour* 135(1):311–319. doi:10.1016/j.jpowsour.2004.03.083
77. Lee CK, Rhee K-I (2002) Preparation of LiCoO₂ from spent lithium-ion batteries. *J Power Sour* 109(1):17–21. doi:10.1016/S0378-7753(02)00037-X
78. Bahgat M, Farghaly F, Basir S, Fouad O (2007) Synthesis, characterization and magnetic properties of microcrystalline lithium cobalt ferrite from spent lithium-ion batteries. *J Mater Process Technol* 183(1):117–121. doi:10.1016/j.jmatprotec.2006.10.005
79. Lain MJ (2001) Recycling of lithium ion cells and batteries. *J Power Sour* 97:736–738. doi:10.1016/S0378-7753(01)00600-0
80. <http://www.recupyl.com/156-hydrometallurgy.html>. Accessed June 2014
81. Zhang P, Yokoyama T, Itabashi O, Suzuki TM, Inoue K (1998) Hydrometallurgical process for recovery of metal values from spent lithium-ion secondary batteries. *Hydrometallurgy* 47(2):259–271. doi:10.1016/S0304-386X(97)00050-9
82. Lupi C, Pasquali M (2003) Electrolytic nickel recovery from lithium-ion batteries. *Miner Eng* 16(6):537–542. doi:10.1016/S0892-6875(03)00080-3
83. Contestabile M, Panero S, Scrosati B (1999) A laboratory-scale lithium battery recycling process. *J Power Sour* 83(1):75–78. doi:10.1016/S0378-7753(99)00261-X
84. Lee CK, Rhee K-I (2003) Reductive leaching of cathodic active materials from lithium ion battery wastes. *Hydrometallurgy* 68(1):5–10. doi:10.1016/S0304-386X(02)00167-6
85. <http://ecobatgroup.com/ecobat/rp/index.php>. Accessed May 2014

86. Sloop SE, Parker R (2011) System and method for processing an end-of-life or reduced performance energy storage and/or conversion device using a supercritical fluid. United States Patent US8067107 B2, November 29, 2011
87. Liu G, Minor A (2012) Pre-lithiated graphite is re-produced by recycling Lithium ion batteries, <http://techtransfer.universityofcalifornia.edu/NCD/22271.html>, United States Patent, Tech ID: 22271/UC Case 2012-074-0
88. Zhang T, He Y, Ge L, Fu R, Zhang X, Huang Y (2013) Characteristics of wet and dry crushing methods in the recycling process of spent lithium-ion batteries. *J Power Sour* 240:766–771. doi:10.1016/j.jpowsour.2013.05.009
89. Xiang D, Wu M, Xu J, Guo J, Chen Y (2012) Detecting method of specific capacity of negative electrode material of lithium ion battery after circulation. China Patent CN102610792-A, July 25, 2012
90. Hamby WD, Slade MD (1978) Process for regenerating and for recovering metallic copper from chloride-containing etching solutions. United States Patent US4252621 A, February 24, 1981
91. Veit HM, Bernardes AM, Ferreira JZ, Tenório JAS, Malfatti CdF (2006) Recovery of copper from printed circuit boards scraps by mechanical processing and electrometallurgy. *J Hazard Mater* 137(3):1704–1709. doi:10.1016/j.jhazmat.2006.05.010
92. Lee M-S, Ahn J-G, Ahn J-W (2003) Recovery of copper, tin and lead from the spent nitric etching solutions of printed circuit board and regeneration of the etching solution. *Hydrometallurgy* 70(1–3):23–29. doi:10.1016/S0304-386X(03)00045-8
93. Fornari P, Abbruzzese C (1999) Copper and nickel selective recovery by electrowinning from electronic and galvanic industrial solutions. *Hydrometallurgy* 52(3):209–222. doi:10.1016/S0304-386X(99)00019-5
94. Botte GG (2012) Removal of metals from water. United States Patent US20120024719 A1, February 2, 2012
95. Ellis TW, Montenegro JA (2013) Magnetic separation of electrochemical cell materials. United States Patent US20130256198, October 3, 2011
96. Nelson P, Gallagher KG, Bloom I, Dees DW (2011) Modeling the performance and cost of lithium-ion batteries for electric-drive vehicles. Argonne National Laboratory (ANL). <http://www.osti.gov/scitech/biblio/1027714>. Accessed Feb 2014
97. Takahashi H (2013) System for recovering solvent vapor e.g. *N*-methyl-2-pyrrolidone (NMP) used at lithium ion battery factory, has heat-use unit that utilizes one portion of heat for heating regeneration of adsorbent of adsorption recovery unit, Japan Patent JP2013111543-A, November 30, 2011
98. Terashi R, Kawata K (2013) System for purifying *N*-methyl-2-pyrrolidone discharged from manufacture of electrode, has apparatus comprising vapor permeable film which selectively permeates moisture content with respect to *N*-methyl-2-pyrrolidone aqueous solution, Japan Patent JP2013018747-A, January 31
99. Kameyama K, Hirose E, Shiraiishi A (2005) Equipment for recovering *N*-methyl-2-pyrrolidone, has several absorption portions filled with filler, in which *N*-methyl-2-pyrrolidone is absorbed to water or aqueous liquid by contacting, Japan Patent JP2005238220-A, December 24, 2004
100. Terashi R, Kawata K (2013) System for purifying *N*-methyl-2-pyrrolidone during manufacture of electrode, has apparatus comprising vapor permeable film having affinity with respect to water and carrying out evaporation of aqueous solution containing pyrrolidone, Japan Patent JP2013018748-A, January 31
101. Noll P, Höpel G, Schroeder M, Passerini S, Winter M From lab scale to large volume production: substitution of toxic NMP/PVDF with H₂O/CMC/SBR in lithium-ion cells. In: 225th ECS Meeting, Orlando Florida, May 15 2014. ECS Meeting Abstracts The Electrochemical Society, p 163
102. Chagnes A, Pospiech B (2013) A brief review on hydrometallurgical technologies for recycling spent lithium-ion batteries. *J Chem Technol Biotechnol* 88(7):1191–1199. doi:10.1002/jctb.4053
103. Agubra V, Fergus J (2013) Lithium ion battery anode aging mechanisms. *Materials* 6(4):1310–1325. doi:10.3390/ma6041310
104. Yoon S, Kim H, Oh SM (2001) Surface modification of graphite by coke coating for reduction of initial irreversible capacity in lithium secondary batteries. *J Power Sour* 94(1):68–73. doi:10.1016/S0378-7753(00)00601-7
105. Safari M, Delacourt C (2011) Aging of a commercial graphite/LiFePO₄ cell. *J Electrochem Soc* 158(10):A1123–A1135. doi:10.1149/1.3614529
106. Sinha NN, Marks TH, Dahn HM, Smith AJ, Burns J, Coyle DJ, Dahn JJ, Dahn J (2012) The rate of active lithium loss from a soft carbon negative electrode as a function of temperature, time and electrode potential. *J Electrochem Soc* 159(10):A1672–A1681. doi:10.1149/2.048210jes
107. Novák P, Joho F, Lanz M, Rykart B, Panitz J-C, Allia D, Kötzer R, Haas O (2001) The complex electrochemistry of graphite electrodes in lithium-ion batteries. *J Power Sour* 97:39–46. doi:10.1016/S0378-7753(01)00586-9
108. Sinha NN, Smith A, Burns JC, Jain G, Eberman K, Scott E, Gardner J, Dahn J (2011) The use of elevated temperature storage experiments to learn about parasitic reactions in wound LiCoO₂/graphite cells. *J Electrochem Soc* 158(11):A1194–A1201. doi:10.1149/2.007111jes
109. Zhu X, Zhu Y, Murali S, Stoller MD, Ruoff RS (2011) Nanostructured reduced graphene oxide/Fe₂O₃ composite as a high-performance anode material for lithium ion batteries. *ACS Nano* 5(4):3333–3338. doi:10.1021/nm200493r
110. Verma P, Novák P (2012) Formation of artificial solid electrolyte interphase by grafting for improving Li-ion intercalation and preventing exfoliation of graphite. *Carbon* 50(7):2599–2614. doi:10.1016/j.carbon.2012.02.019
111. Botte GG (2005) Modeling volume changes due to lithium intercalation in a carbon fiber. *Electrochim Acta* 50(28):5647–5658. doi:10.1016/j.electacta.2005.03.058
112. Yuqin C, Hong L, Lie W, Tianhong L (1997) Irreversible capacity loss of graphite electrode in lithium-ion batteries. *J Power Sour* 68(2):187–190. doi:10.1016/S0378-7753(96)02549-9
113. Simon B, Flandrois S, Guerin K, Fevrier-Bouvier A, Teulat I, Biensan P (1999) On the choice of graphite for lithium ion batteries. *J Power Sour* 81:312–316. doi:10.1016/S0378-7753(99)00211-6
114. Zheng H, Ridgway P, Song X, Xun S, Chong J, Liu G, Battaglia V (2011) Comparison of cycling performance of lithium ion cell anode graphites. *Electrochem Soc Trans* 33(29):91–100. doi:10.1149/2.006205jes
115. Andersson AM, Edström K, Thomas JO (1999) Characterisation of the ambient and elevated temperature performance of a graphite electrode. *J Power Sour* 81:8–12. doi:10.1016/S0378-7753(99)00185-8
116. Peled E, Golodnitsky D, Penciner J (2011) The anode/electrolyte interface. In: *Handbook of battery materials*. Wiley, KGaA, pp 479–523. doi:10.1002/9783527637188.ch16
117. Aurbach D, Markovsky B, Weissman I, Levi E, Ein-Eli Y (1999) On the correlation between surface chemistry and performance of graphite negative electrodes for Li ion batteries. *Electrochim Acta* 45:67–86. doi:10.1016/S0013-4686(99)00194-2
118. Dey AN, Sullivan BP (1970) The electrochemical decomposition of propylene carbonate on graphite. *J Electrochem Soc* 117(2):222–224. doi:10.1149/1.2407470
119. Ra Fong, von Sacken U, Dahn JR (1990) Studies of lithium intercalation into carbons using nonaqueous electrochemical

- cells. *J Electrochem Soc* 137(7):2009–2013. doi:10.1149/1.2086855
120. Shu ZX, McMillan RS, Murray JJ (1993) Electrochemical Intercalation of lithium into graphite. *J Electrochem Soc* 140(4):922–927. doi:10.1149/1.2056228
 121. Aurbach D, Ein-Eli Y, Chusid O, Carmeli Y, Babai M, Yamin H (1994) The correlation between the surface chemistry and the performance of Li-carbon intercalation anodes for rechargeable ‘rocking-chair’ type batteries. *J Electrochem Soc* 141(3):603–611. doi:10.1149/1.2054777
 122. Besenhard JO, Winter M, Yang J, Biberacher W (1995) Filming mechanism of lithium-carbon anodes in organic and inorganic electrolytes. *J Power Sour* 54(2):228–231. doi:10.1016/0378-7753(94)02073-C
 123. Komaba S, Kaplan B, Ohtsuka T, Kataoka Y, Kumagai N, Groult H (2003) Inorganic electrolyte additives to suppress the degradation of graphite anodes by dissolved Mn(II) for lithium-ion batteries. *J Power Sour* 119–121:378–382. doi:10.1016/S0378-7753(03)00224-6
 124. Zhang SS (2006) A review on electrolyte additives for lithium-ion batteries. *J Power Sour* 162(2):1379–1394. doi:10.1016/j.jpowsour.2006.07.074
 125. Liu Z, Yu A, Lee JY (1999) Modifications of synthetic graphite for secondary lithium-ion battery applications. *J Power Sour* 81–82:187–191. doi:10.1016/S0378-7753(98)00243-2
 126. Bourlinos AB, Gournis D, Petridis D, Szabó T, Szeri A, Dékány I (2003) Graphite oxide: chemical reduction to graphite and surface modification with primary aliphatic amines and amino acids. *Langmuir* 19(15):6050–6055. doi:10.1021/la026525h
 127. Li H, Zhou H (2011) Enhancing the performances of Li-ion batteries by carbon-coating: present and future. *Chem Commun* 48(9):1201–1217. doi:10.1039/c1cc14764a
 128. Wu YP, Jiang C, Wan C, Holze R (2002) Modified natural graphite as anode material for lithium ion batteries. *J Power Sour* 111(2):329–334. doi:10.1016/S0378-7753(02)00349-X
 129. Peled E, Golodnitsky D, Ullus A, Yufit V (2004) Effect of carbon substrate on SEI composition and morphology. *Electrochim Acta* 50(2–3):391–395. doi:10.1016/j.electacta.2004.01.130
 130. Spahr ME, Buqa H, Würsig A, Goers D, Hardwick L, Novák P, Krumeich F, Dentzer J, Vix-Guterl C (2006) Surface reactivity of graphite materials and their surface passivation during the first electrochemical lithium insertion. *J Power Sour* 153(2):300–311. doi:10.1016/j.jpowsour.2005.05.032
 131. Winter M, Novák P, Monnier A (1998) Graphites for lithium-ion cells: the correlation of the first-cycle charge loss with the Brunauer–Emmett–Teller surface area. *J Electrochem Soc* 145(2):428–436. doi:10.1149/1.1838281
 132. Ng SH, Vix-Guterl C, Bernardo P, Tran N, Ufheil J, Buqa H, Dentzer J, Gadiou R, Spahr ME, Goers D, Novák P (2009) Correlations between surface properties of graphite and the first cycle specific charge loss in lithium-ion batteries. *Carbon* 47(3):705–712. doi:10.1016/j.carbon.2008.11.008
 133. Novák P, Ufheil J, Buqa H, Krumeich F, Spahr ME, Goers D, Wilhelm H, Dentzer J, Gadiou R, Vix-Guterl C (2007) The importance of the active surface area of graphite materials in the first lithium intercalation. *J Power Sour* 174(2):1082–1085. doi:10.1016/j.jpowsour.2007.06.036
 134. Chung GC, Jun SH, Lee KY, Kim MH (1999) Effect of surface structure on the irreversible capacity of various graphitic carbon electrodes. *J Electrochem Soc* 146(5):1664–1671. doi:10.1149/1.1391823
 135. Wang H-Y, Wang F-M (2013) Electrochemical investigation of an artificial solid electrolyte interface for improving the cyclability of lithium ion batteries using an atomic layer deposition on a graphite electrode. *J Power Sour* 233:1–5. doi:10.1016/j.jpowsour.2013.01.134
 136. Peled E, Menachem C, Bar-Tow D, Melman A (1996) Improved graphite anode for lithium-ion batteries chemically: bonded solid electrolyte interface and nanochannel formation. *J Electrochem Soc* 143(1):L4–L7. doi:10.1149/1.1836372
 137. Wu YP, Jiang C, Wan C, Holze R (2003) Anode materials for lithium ion batteries by oxidative treatment of common natural graphite. *Solid State Ion* 156(3–4):283–290. doi:10.1016/S0167-2738(02)00680-X
 138. Spahr ME, Wilhelm H, Joho F, Panitz J-C, Wambach J, Novák P, Dupont-Pavlovsky N (2002) Purely hexagonal graphite and the influence of surface modifications on its electrochemical lithium insertion properties. *J Electrochem Soc* 149(8):A960–A966. doi:10.1149/1.1486238
 139. Yu P, Ritter JA, White RE, Popov BN (2000) Ni-composite microencapsulated graphite as the negative electrode in lithium-ion batteries II: electrochemical impedance and self-discharge studies. *J Electrochem Soc* 147(6):2081–2085. doi:10.1149/1.1393489
 140. Yu P, Ritter JA, White RE, Popov BN (2000) Ni-composite microencapsulated graphite as the negative electrode in lithium-ion batteries I. Initial irreversible capacity study. *J Electrochem Soc* 147(4):1280–1285. doi:10.1149/1.1393350
 141. Shi L, Wang Q, Li H, Wang Z, Huang X, Chen L (2001) Electrochemical performance of Ni-deposited graphite anodes for lithium secondary batteries. *J Power Sour* 102(1–2):60–67. doi:10.1016/S0378-7753(01)00773-X
 142. Takamura T, Sumiya K, Suzuki J, Yamada C, Sekine K (1999) Enhancement of Li doping/undoping reaction rate of carbonaceous materials by coating with an evaporated metal film. *J Power Sour* 81–82:368–372. doi:10.1016/S0378-7753(98)00220-1
 143. Veeraraghavan B, Durairajan A, Haran B, Popov B, Guidotti R (2002) Study of Sn-coated graphite as anode material for secondary lithium-ion batteries. *J Electrochem Soc* 149(6):A675–A681. doi:10.1149/1.1470653
 144. Lee JY, Zhang R, Liu Z (2000) Dispersion of Sn and SnO on carbon anodes. *J Power Sour* 90(1):70–75. doi:10.1016/S0378-7753(00)00450-X
 145. Momose H, Honbo H, Takeuchi S, Nishimura K, Horiba T, Muranaka Y, Kozono Y, Miyadera H (1997) X-ray photoelectron spectroscopy analyses of lithium intercalation and alloying reactions on graphite electrodes. *J Power Sour* 68(2):208–211. doi:10.1016/S0378-7753(96)02627-4
 146. Nishimura K, Honbo H, Takeuchi S, Horiba T, Oda M, Koseki M, Muranaka Y, Kozono Y, Miyadera H (1997) Design and performance of 10 Wh rechargeable lithium batteries. *J Power Sour* 68(2):436–439. doi:10.1016/S0378-7753(97)02534-2
 147. Kim S-S, Kadoma Y, Ikuta H, Uchimoto Y, Wakihara M (2001) Electrochemical performance of natural graphite by surface modification using aluminum. *Electrochem Solid-State Lett* 4(8):A109–A112. doi:10.1149/1.1379829
 148. Wu Y, Jiang C, Wan C, Tsuchida E (2000) Composite anode material for lithium ion battery with low sensitivity to water. *Electrochem Commun* 2(9):626–629. doi:10.1016/S1388-2481(00)00091-6
 149. Wu YP, Jiang C, Wan C, Holze R (2002) Composite materials of silver and natural graphite as anode with low sensibility to humidity. *J Power Sour* 112(1):255–260. doi:10.1016/S0378-7753(02)00392-0
 150. Lee JK, Ryu DH, Ju JB, Shul YG, Cho BW, Park D (2002) Electrochemical characteristics of graphite coated with tin-oxide and copper by fluidised-bed chemical vapour deposition. *J Power Sour* 107(1):90–97. doi:10.1016/S0378-7753(01)00985-5
 151. Huang H, Kelder EM, Schoonman J (2001) Graphite-metal oxide composites as anode for Li-ion batteries. *J Power Sour* 97–98:114–117. doi:10.1016/S0378-7753(01)00597-3

152. Jung YS, Cavanagh AS, Riley LA, Kang S-H, Dillon AC, Groner MD, George SM, Lee S-H (2010) Ultrathin direct atomic layer deposition on composite electrodes for highly durable and safe Li-ion batteries. *Adv Mater* 22(19):2172–2176. doi:10.1002/adma.200903951
153. Lee S-E, Kim E, Cho J (2007) Improvement of electrochemical properties of natural graphite anode materials with an ovoid morphology by AlPO_4 coating. *Electrochem Solid-State Lett* 10(1):A1–A4. doi:10.1149/1.2364308
154. Veeraraghavan B, Paul J, Haran B, Popov B (2002) Study of polypyrrole graphite composite as anode material for secondary lithium-ion batteries. *J Power Sour* 109(2):377–387. doi:10.1016/S0378-7753(02)00105-2
155. Pan Q, Guo K, Wang L, Fang S (2002) Ionic conductive copolymer encapsulated graphite as an anode material for lithium ion batteries. *Solid State Ionics* 149(3–4):193–200. doi:10.1016/S0167-2738(02)00278-3
156. Guo K, Pan Q, Fang S (2002) Poly(acrylonitrile) encapsulated graphite as anode materials for lithium ion batteries. *J Power Sour* 111(2):350–356. doi:10.1016/S0378-7753(02)00347-6
157. Wang H, Yoshio M (2001) Carbon-coated natural graphite prepared by thermal vapor decomposition process, a candidate anode material for lithium-ion battery. *J Power Sour* 93(1–2):123–129. doi:10.1016/S0378-7753(00)00552-8
158. Lee H-Y, Baek J-K, Jang S-W, Lee S-M, Hong S-T, Lee K-Y, Kim M-H (2001) Characteristics of carbon-coated graphite prepared from mixture of graphite and polyvinylchloride as anode materials for lithium ion batteries. *J Power Sour* 101(2):206–212. doi:10.1016/S0378-7753(01)00671-1
159. Ito S, Nakaoka K, Kawamura M, Ui K, Fujimoto K, Koura N (2005) Lithium battery having a large capacity using Fe_3O_4 as a cathode material. *J Power Sour* 146:319–322. doi:10.1016/j.jpowsour.2005.03.130
160. Mitra S, Poizot P, Finke A, Tarascon JM (2006) Growth and electrochemical characterization versus lithium of Fe_3O_4 electrodes made by electrodeposition. *Adv Funct Mater* 16(17):2281–2287. doi:10.1002/adfm.200500753
161. Taberna PL, Mitra S, Poizot P, Simon P, Tarascon JM (2006) High rate capabilities Fe_3O_4 -based Cu nano-architected electrodes for lithium-ion battery applications. *Nat Mater* 5(7):567–573. doi:10.1038/nmat1672
162. Zhang W-M, Wu X-L, Hu J-S, Guo Y-G, Wan L-J (2008) Carbon coated Fe_3O_4 nanoparticles as a superior anode material for lithium-ion batteries. *Adv Funct Mater* 18(24):3941–3946. doi:10.1002/adfm.200801386
163. Muraliganth T, Vadivel Murugan A, Manthiram A (2009) Facile synthesis of carbon-decorated single-crystalline Fe_3O_4 nanowires and their application as high performance anode in lithium ion batteries. *Chem Commun* 47:7360–7362. doi:10.1039/b916376j
164. Liu H, Wang G, Wang J, Wexler D (2008) Magnetite/carbon core-shell nanorods as anode materials for lithium-ion batteries. *Electrochem Commun* 10(12):1879–1882. doi:10.1016/j.elecom.2008.09.036
165. Liu J, Li Y, Fan H, Zhu Z, Jiang J, Ding R, Hu Y, Huang X (2010) Iron oxide-based nanotube arrays derived from sacrificial template-accelerated hydrolysis: large-area design and reversible lithium storage. *Chem Mater* 22(1):212–217. doi:10.1021/cm903099w
166. Zhu T, Chen JS, Lou XW (2011) Glucose-assisted one-pot synthesis of FeOOH nanorods and their transformation to Fe_3O_4 @carbon nanorods for application in lithium ion batteries. *J Phys Chem C* 115(19):9814–9820. doi:10.1021/jp2013754
167. Chen JS, Zhang Y, Lou XW (2011) One-pot synthesis of uniform Fe_3O_4 nanospheres with carbon matrix support for improved lithium storage capabilities. *ACS Appl Mater Interfaces* 3(9):3276–3279. doi:10.1021/am201079z
168. Kang N, Park JH, Choi J, Jin J, Chun J, Jung IG, Jeong J, Park J-G, Lee SM, Kim HJ, Son SU (2012) Nanoparticulate iron oxide tubes from microporous organic nanotubes as stable anode materials for lithium ion batteries. *Angew Chem Int Ed* 51(27):6626–6630. doi:10.1002/anie.201202244
169. Wang Z, Zhou L, Lou XW (2012) Metal oxide hollow nanostructures for lithium-ion batteries. *Adv Mater* 24(14):1903–1911. doi:10.1002/adma.201200469
170. Cui Z-M, Jiang L-Y, Song W-G, Guo Y-G (2009) High-yield gas-liquid interfacial synthesis of highly dispersed Fe_3O_4 nanocrystals and their application in lithium-ion batteries. *Chem Mater* 21(6):1162–1166. doi:10.1021/cm8033609
171. Zhou G, Wang D-W, Li F, Zhang L, Li N, Wu Z-S, Wen L, Lu GQ, Cheng H-M (2010) Graphene-wrapped Fe_3O_4 anode material with improved reversible capacity and cyclic stability for lithium ion batteries. *Chem Mater* 22(18):5306–5313. doi:10.1021/cm101532x
172. Arico AS, Bruce P, Scrosati B, Tarascon J-M, van Schalkwijk W (2005) Nanostructured materials for advanced energy conversion and storage devices. *Nat Mater* 4(5):366–377. doi:10.1038/nmat1368
173. Guo Y-G, Hu J-S, Wan L-J (2008) Nanostructured materials for electrochemical energy conversion and storage devices. *Adv Mater* 20(15):2878–2887. doi:10.1002/adma.200800627
174. He C, Wu S, Zhao N, Shi C, Liu E, Li J (2013) Carbon-encapsulated Fe_3O_4 nanoparticles as a high-rate lithium ion battery Anode material. *ACS Nano* 7(5):4459–4469. doi:10.1021/nn401059h
175. Poizot P, Laruelle S, Grugeon S, Dupont L, Tarascon JM (2000) Nano-sized transition-metal oxides as negative-electrode materials for lithium-ion batteries. *Nature* 407(6803):496–499. doi:10.1038/35035045
176. Lou XW, Wang Y, Yuan C, Lee JY, Archer LA (2006) Template-free synthesis of SnO_2 hollow nanostructures with high lithium storage capacity. *Adv Mater* 18(17):2325–2329. doi:10.1002/adma.200600733
177. Jiao F, Bruce PG (2007) Mesoporous crystalline $\beta\text{-MnO}_2$ —a reversible positive electrode for rechargeable lithium batteries. *Adv Mater* 19(5):657–660. doi:10.1002/adma.200602499
178. Delmer O, Balaya P, Kienle L, Maier J (2008) Enhanced potential of amorphous electrode materials: case study of RuO_2 . *Adv Mater* 20(3):501–505. doi:10.1002/adma.200701349
179. Dominko R, Goupil JM, Bele M, Gaberscek M, Remskar M, Hanzel D, Jamnik J (2005) Impact of LiFePO_4/C composites porosity on their electrochemical performance. *J Electrochem Soc* 152(5):A858–A863. doi:10.1149/1.1872674
180. Cao Q, Zhang HP, Wang GJ, Xia Q, Wu YP, Wu HQ (2007) A novel carbon-coated LiCoO_2 as cathode material for lithium ion battery. *Electrochem Commun* 9(5):1228–1232. doi:10.1016/j.elecom.2007.01.017
181. Hu YS, Guo YG, Dominko R, Gaberscek M, Jamnik J, Maier J (2007) Improved electrode performance of porous LiFePO_4 using RuO_2 as an oxidic nanoscale interconnect. *Adv Mater* 19(15):1963–1966. doi:10.1002/adma.200700697
182. Hu J, Li H, Huang X, Chen L (2006) Improve the electrochemical performances of Cr_2O_3 anode for lithium ion batteries. *Solid State Ionics* 177(26–32):2791–2799. doi:10.1016/j.ssi.2006.03.043
183. Aurbach D, Levi MD, Levi E, Schechter A (1997) Failure and stabilization mechanisms of graphite electrodes. *J Phys Chem B* 101(12):2195–2206. doi:10.1021/jp962815t
184. Needham SA, Wang GX, Konstantinov K, Tournayre Y, Lao Z, Liu HK (2006) Electrochemical performance of $\text{Co}_3\text{O}_4/\text{C}$

- composite anode materials. *Electrochem Solid-State Lett* 9(7):A315–A319. doi:[10.1149/1.2197108](https://doi.org/10.1149/1.2197108)
185. Zaghbi K, Nadeau G, Kinoshita K (2001) Influence of edge and basal plane sites on the electrochemical behavior of flake-like natural graphite for Li-ion batteries. *J Power Sour* 97:97–103. doi:[10.1016/S0378-7753\(01\)00596-1](https://doi.org/10.1016/S0378-7753(01)00596-1)
186. Kim T-H, Jeon EK, Ko Y, Jang BY, Kim B-S, Song H-K (2014) Enlarging the d-spacing of graphite and polarizing its surface charge for driving lithium ions fast. *J Mater Chem A* 2(20):7600–7605. doi:[10.1039/c3ta15360f](https://doi.org/10.1039/c3ta15360f)